

Targeting STING with covalent small-molecule inhibitors

Simone M. Haag^{1,4}, Muhammet F. Gulen^{1,4}, Luc Reymond², Antoine Gibelin², Laurence Abrami¹, Alexiane Decout¹, Michael Heymann¹, F. Gisou van der Goot¹, Gerardo Turcatti², Rayk Behrendt³ & Andrea Ablasser^{1,*}

Aberrant activation of innate immune pathways is associated with a variety of diseases. Progress in understanding the molecular mechanisms of innate immune pathways has led to the promise of targeted therapeutic approaches, but the development of drugs that act specifically on molecules of interest remains challenging. Here we report the discovery and characterization of highly potent and selective small-molecule antagonists of the stimulator of interferon genes (STING) protein, which is a central signalling component of the intracellular DNA sensing pathway^{1,2}. Mechanistically, the identified compounds covalently target the predicted transmembrane cysteine residue 91 and thereby block the activation-induced palmitoylation of STING. Using these inhibitors, we show that the palmitoylation of STING is essential for its assembly into multimeric complexes at the Golgi apparatus and, in turn, for the recruitment of downstream signalling factors. The identified compounds and their derivatives reduce STING-mediated inflammatory cytokine production in both human and mouse cells. Furthermore, we show that these small-molecule antagonists attenuate pathological features of autoinflammatory disease in mice. In summary, our work uncovers a mechanism by which STING can be inhibited pharmacologically and demonstrates the potential of therapies that target STING for the treatment of autoinflammatory disease.

STING is an intracellular signalling molecule that senses cyclic dinucleotides from bacterial sources or cyclic GMP–AMP (2′-3′)—produced by the cytosolic DNA sensor cyclic GMP–AMP synthase—and, upon stimulation, triggers the production of type I interferons (IFNs) and other inflammatory mediators^{1,3–10}. Chronic activation of STING has previously been implicated in the pathogenesis of monogenic autoinflammatory conditions, such as Aicardi–Goutières syndrome and STING-associated vasculopathy with onset in infancy^{11–14}. In addition, accumulating evidence suggests a pathogenic role for STING in a range of more complex inflammatory diseases^{15–20}. Thus, STING represents an attractive target for therapeutic intervention.

To discover molecules that inhibit STING, we performed a cell-based chemical screen and identified two nitrofuran derivatives—C-178 and C-176—that strongly reduced STING-mediated, but not RIG-I- or TBK1-mediated, IFN β reporter activity (Fig. 1a, b and Extended Data Fig. 1a–d). A limited structure–activity relationship analysis revealed that both the nitro group and the furan moiety were essential for the bioactivity of the compounds, and that substituents at the 4-position of the phenyl ring fine-tuned their inhibitory potency (Extended Data Fig. 1e, f). Studies in mouse bone marrow-derived macrophages (BMDMs) corroborated the finding that C-178 potently and selectively suppressed the STING responses elicited by distinct bona fide activators (Fig. 1c–e and Extended Data Fig. 2a, b). Profiling the effect of C-178 on the global transcriptional program initiated by the STING agonist 10-carboxymethyl-9-acridanone (CMA) in BMDMs showed a substantial reduction of 99.6% (498) of the 500 most-upregulated genes (Extended Data Fig. 2c, d). Of note, exposure to C-178 alone did not

appreciably affect the gene expression profile of BMDMs relative to DMSO-treated samples. In addition, C-178 inhibited the CMA-induced phosphorylation of TBK1, a key downstream protein kinase of STING (Fig. 1f). Notably, however, C-178 did not appreciably affect STING responses in human cells (Extended Data Fig. 2e). The species-specific activity of C-178 and C-176 suggested that the compounds directly target mouse STING (mmSTING) but not human STING (hsSTING).

5,6-Dimethylxanthenone-4-acetic acid (DMXAA) and CMA, which are mouse-specific activators of STING, have previously been described as acting through non-conserved amino acid residues located within the C-terminal region of mmSTING that encompass the ligand-binding domain^{21,22}. However, using chimaeric STING expression constructs we found that C-178 targeted the poorly characterized N-terminal portion of mmSTING that includes the transmembrane domains (Extended Data Fig. 2f). To map the amino acids involved in the inhibitory activity of C-178, we individually mutated several amino acids (alanine-scanning) located in the N-terminal part of mmSTING (amino acids 21–137) and screened for mutants with compromised sensitivity to C-178. A STING mutant with a Cys91-to-alanine replacement (STING(C91A)) was found to be entirely resistant to inhibition by C-178 (Fig. 2a, b). Based on the critical roles of both the nucleophilic cysteine residue on mmSTING and the electrophilic nitrofur group of the compounds, we hypothesized that a covalent bond may be formed between C-178 and Cys91. Indeed, cellular washout experiments, native mass spectrometry assays on mmSTING (wild type and STING(C91S)) and top-down liquid-chromatography tandem mass spectrometry (LC-MS/MS) together confirmed that the Cys91 of mmSTING is covalently modified by C-178 and C-176 (Fig. 2c, Extended Data Fig. 3 and Supplementary Information).

To further characterize the binding of the compounds to mmSTING, we performed gel-based profiling studies using a derivative of C-176 with an installed alkyne group (C-176-AL), which is amenable to copper-catalysed azide alkyne cycloaddition (click chemistry) (Extended Data Fig. 4a, b). We found that within living cells C-176-AL effectively and specifically labelled mmSTING, whereas neither hsSTING nor mmSTING with a Cys91 substitution (either STING(C91A) or STING(C91S)) were targeted by the clickable compound (Fig. 2d, e and Extended Data Fig. 4c–e). We then used the gel-based protein profiling approach to study the degree of molecular selectivity in the covalent interaction between the compounds and STING. When compared to iodacetamide azide, which is a non-specific cross-linking probe, an azide-based clickable C-176 probe (C-176-AZ) showed markedly lower background proteome reactivity (Extended Data Fig. 4f). Furthermore, testing STING against a panel of proteins that contain hyper-reactive cysteine residues revealed that only STING was efficiently labelled by C-176-AZ^{23,24} (Extended Data Fig. 4g). We also note that the installation of an additional methyl group at the central amine moiety of C-176 completely abolished the inhibitory capacity of the compound (Extended Data Fig. 1e, f). Collectively, these studies provide evidence that the nitrofur scaffold does not randomly cross-react with cellular

¹Global Health Institute, Swiss Federal Institute of Technology Lausanne (EPFL), Lausanne, Switzerland. ²Biomolecular Screening Facility, Swiss Federal Institute of Technology Lausanne (EPFL), Lausanne, Switzerland. ³Institute for Immunology, Faculty of Medicine, Technical University Dresden, Dresden, Germany. ⁴These authors contributed equally: Simone M. Haag, Muhammet F. Gulen. *e-mail: andrea.ablasser@epfl.ch

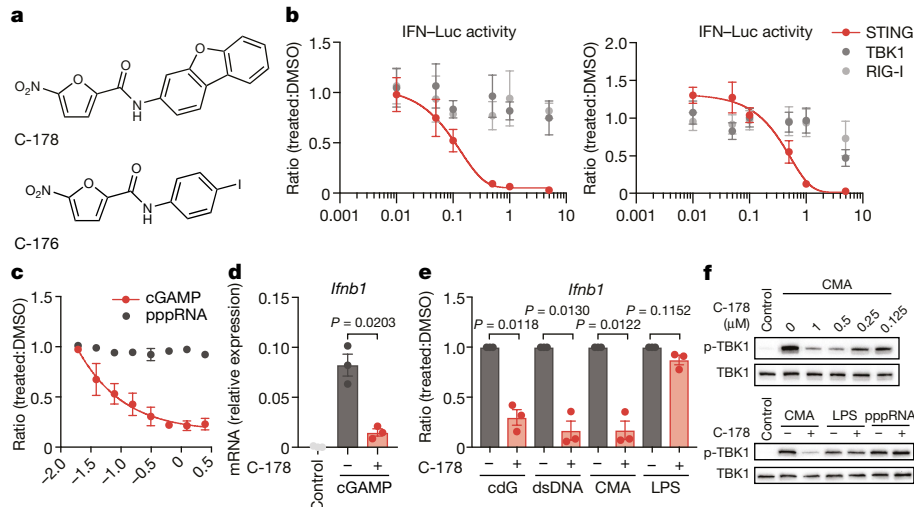


Fig. 1 | Identification of small-molecule inhibitors of STING.

a, C-176 and C-178. **b**, IFN β luciferase reporter activity in HEK293T cells, transfected as indicated (compound concentration 0.01–5 μ M) ($n = 3$ biological replicates). **c**, Type I IFN bioassay of BMDMs with or without C-178 (0.02–2.5 μ M) ($n = 3$ biological replicates). cGAMP, cyclic GMP–AMP (2'-3'); pppRNA, 5'-triphosphate RNA. **d**, **e**, *Ifnb1* expression levels

in BMDMs treated with C-178 (0.5 μ M) ($n = 3$ biological replicates). cdG, cyclic di-GMP; dsDNA, double-strand DNA; LPS, lipopolysaccharide. **f**, Immunoblot of phosphorylated TBK1 (p-TBK1) and TBK1 of BMDMs (one representative of $n = 3$ biological replicates). Data are mean \pm s.e.m. *P* values were calculated using two-tailed *t*-test. Nonlinear regression analysis is shown in **b**, **c**. For gel source data, see Supplementary Fig. 1.

proteins, but instead relies on a specific recognition event on STING that precedes the irreversible modification of Cys91. Moreover, the covalent bond between C-178 and STING may be formed by a nucleophilic addition of a nucleophilic side chain of Cys91 to the 4-position of the furan ring, followed by a subsequent intramolecular rearrangement (Fig. 2f and Extended Data Fig. 4h).

We next aimed to understand how the modification introduced by C-178 could antagonize STING. To activate TBK1, STING translocates from the endoplasmic reticulum to the Golgi apparatus^{1,25}. C-178, however, neither impaired the trafficking of STING to the

Golgi apparatus nor affected the endolysosomal degradation of STING thereafter (Fig. 3a, b and Extended Data Fig. 5a, b). We then considered the possibility that C-178 may alter post-translational modifications of STING. We focused on palmitoylation, because this had previously been reported to rely on Cys91 and to be involved in the activation of TBK1²⁶. Indeed, we found that CMA-induced palmitoylation of STING was markedly attenuated in the presence of C-178, but that the palmitoylation of transferrin receptor or calnexin was not affected (Fig. 3c and Extended Data Fig. 5c–e). The exact mechanism through which palmitoylation regulates STING signalling is unclear,

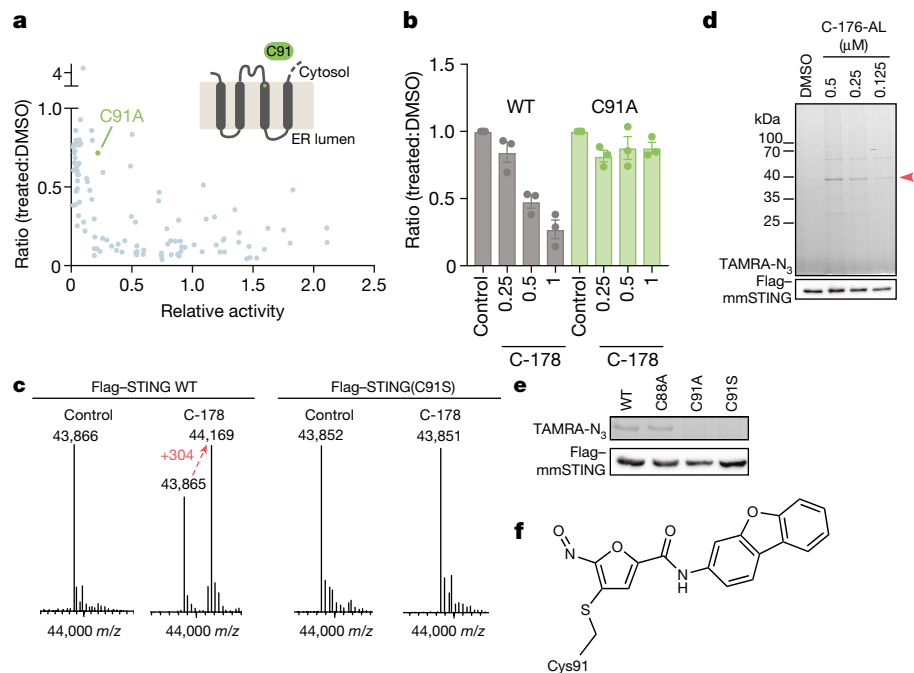


Fig. 2 | Inhibition of STING through covalent binding of C-178 to Cys91. **a**, Alanine scanning on mmSTING (amino acids 21–137). ER, endoplasmic reticulum. **b**, IFN β luciferase reporter measurements of HEK293T cells transfected with mmSTING constructs as indicated, with or without C-178. Data are mean \pm s.e.m. ($n = 3$ biological replicates). WT, wild type. **c**, Deconvoluted electrospray ionization mass spectra for Flag–mmSTING

purified from treated cells, as indicated. **d**, Gel showing labelling events of C-176-AL in HEK293T cells expressing Flag–mmSTING. TAMRA-N₃, tetramethylrhodamine azide. **e**, Gel showing labelling of Flag–mmSTING constructs by C-176-AL (0.25 μ M) in HEK293T cells. **f**, Proposed reaction adduct. One representative of $n = 2$ (**c**) or $n = 3$ (**d**, **e**) biological replicates. For gel source data, see Supplementary Fig. 1.

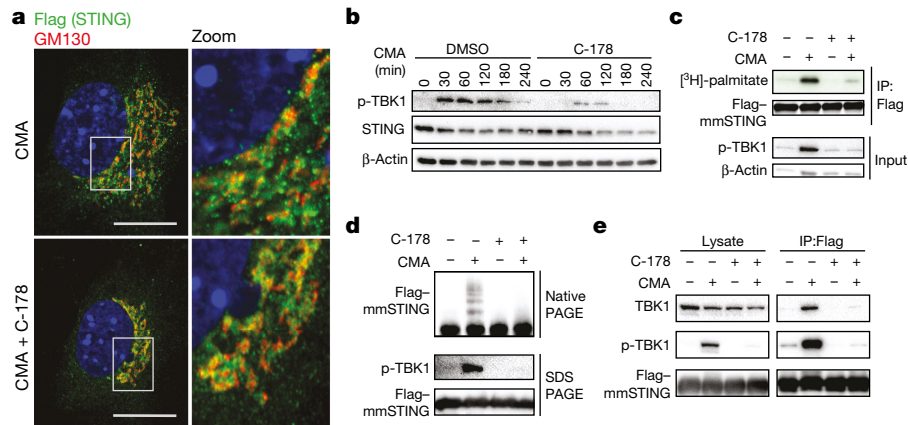


Fig. 3 | C-178 blocks palmitoylation-induced clustering of STING.

a, Staining of Flag (green), GM130 (red) and nuclei (DAPI) in mouse embryonic fibroblasts treated with CMA and expressing Flag–mmSTING (C-178 (1.5 μ M)). Scale bar, 20 μ m. **b**, Immunoblot of p-TBK1, STING and β -actin in mouse embryonic fibroblasts (C-178 (1 μ M)). **c**, [3 H]-palmitate incorporation of Flag–mmSTING in HEK293T cells and protein levels

(p-TBK1 and β -actin) after stimulation with CMA (2 h) (C-178 (1 μ M)). **d**, Blue native PAGE and SDS-PAGE of HEK293T cells with Flag–mmSTING after stimulation with CMA (C-178 (1 μ M)). **e**, Immunoprecipitation from Flag–mmSTING HEK293T cells and detection of TBK1 and p-TBK1 by immunoblotting. One representative of $n = 3$ biological replicates (**a–e**). For gel source data, see Supplementary Fig. 1.

as is the molecular event on STING that enables the recruitment of TBK1. We hypothesized that both of these processes may be connected and explain the mechanism through which C-178 inhibits STING. We observed that, after activation by CMA, STING assembles into clusters, which is a well-known effect of protein palmitoylation (Fig. 3d). Treatment of cells with C-178, C-176 or 2-bromopalmitate—which is a non-selective inhibitor of palmitoylation—completely prevented the formation of STING clusters (Fig. 3d and Extended Data Fig. 5f). Moreover, the clustering of STING paralleled the recruitment and phosphorylation of TBK1, which again was abrogated in the presence of C-178 (Fig. 3e and Extended Data Fig. 5g). Together, this suggests that palmitoylation triggers the assembly of a multimeric complex that enables STING to interact with TBK1. Moreover, C-178 interferes with this process by inhibiting the palmitoylation of STING (Supplementary Note 1).

We next studied the effects of pharmacological inhibition of STING in mice. Because we noticed improved solubility of C-176 relative to C-178, we chose this compound for in vivo studies. First we verified that the compounds target STING by using an in vivo click-chemistry approach and also assessed the pharmacokinetic profile of C-176 on single-dose intraperitoneal injection (Extended Data Fig. 6a, b). We next evaluated whether C-176 can suppress the induction of type I IFNs triggered by the administration of CMA. Of note, pretreatment with C-176 markedly reduced the CMA-mediated induction of serum levels of type I IFNs and IL-6. (Fig. 4a and Extended Data Fig. 6c). Thus, C-176 is effective in mice and—as expected for a covalent inhibitor—the short serum half-life does not limit its in vivo inhibitory capacity. To assess the potential of C-176 to antagonize STING in a model of autoinflammatory disease, we investigated its efficacy in *Trex1*^{−/−} mice. *Trex1*^{−/−} mice show signs of severe multi-organ inflammation caused by the persistent activation of the cyclic GMP–AMP synthase–STING pathway and recapitulate certain pathogenic features of Aicardi–Goutières syndrome in humans^{11,14,27–29}. Having verified that C-178 suppresses interferon-stimulated genes in cells from *Trex1*^{−/−} mice (Extended Data Fig. 7a), we performed a two-week in vivo efficacy study with C-176. Notably, treatment of *Trex1*^{−/−} mice with C-176 resulted in a significant reduction in serum levels of type I IFNs and in a strong suppression of inflammatory parameters in the heart (Extended Data Fig. 7b, c). Wild-type mice on a two-week treatment with C-176 showed no evident signs of overt toxicity (Extended Data Fig. 6d–g). We next conducted a three-month trial with C-176 in *Trex1*^{−/−} mice, which demonstrated marked amelioration of various signs of systemic inflammation (Fig. 4b, c and Extended Data Fig. 7e). Thus, C-176 attenuates STING-associated autoinflammatory disease in mice.

Given that the palmitate-modified cysteines are conserved residues and equally important for the functionality of hsSTING, we next searched for compounds that are capable of inhibiting the human protein. Further derivatization of the C-176 and C-178 scaffold yielded two structurally related compounds—C-170 and C-171—that efficiently inhibited both hsSTING and mmSTING through the same mechanism of action as that detailed above (Extended Data Fig. 8 and Supplementary Information). Encouraged by these results, we aimed to identify a more advanced covalent antagonist of hsSTING and performed another chemical screen. Progression of candidate hits through counter screens and validation screens identified H-151 (Fig. 5a). H-151 potently inhibited hsSTING, as evidenced by abrogation of type I IFN responses, reduction of TBK1 phosphorylation and suppression of hsSTING palmitoylation without affecting respective controls (Fig. 5b–e and Extended Data Fig. 9c). Using an alkyne analogue of

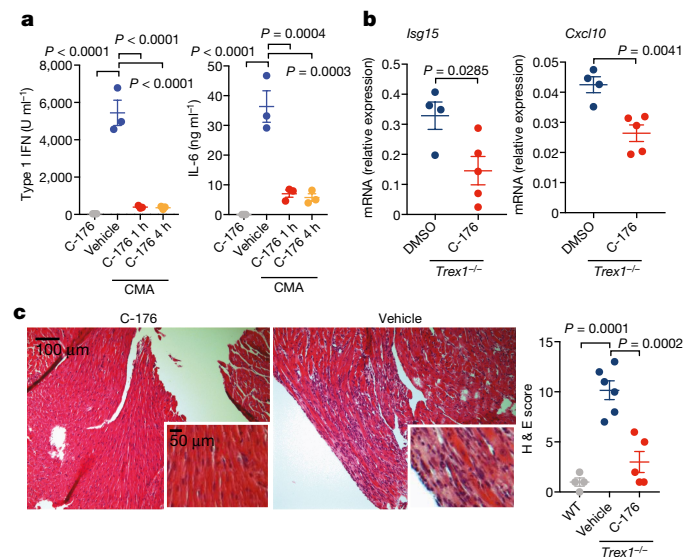


Fig. 4 | In vivo effects of C-176. **a**, Serum levels of type I IFNs and IL-6 from wild-type mice treated with C-176 (for 1 h and 4 h) and stimulated with CMA ($n = 3$ mice). **b**, **c**, Levels of *Isg15* and *Cxcl10* mRNA in the heart of *Trex1*^{−/−} mice (C-176 $n = 5$ and vehicle $n = 4$ mice) and heart histological analysis of wild-type ($n = 4$) or *Trex1*^{−/−} mice (C-176 $n = 5$ and vehicle $n = 6$ mice) treated for three months. H & E, haematoxylin and eosin. Data are mean \pm s.e.m. P values calculated using one-way ANOVA (**a**, **c**) or two-tailed t -test (**b**). Representative image shown in **c**. For source data, see Supplementary Table 1.

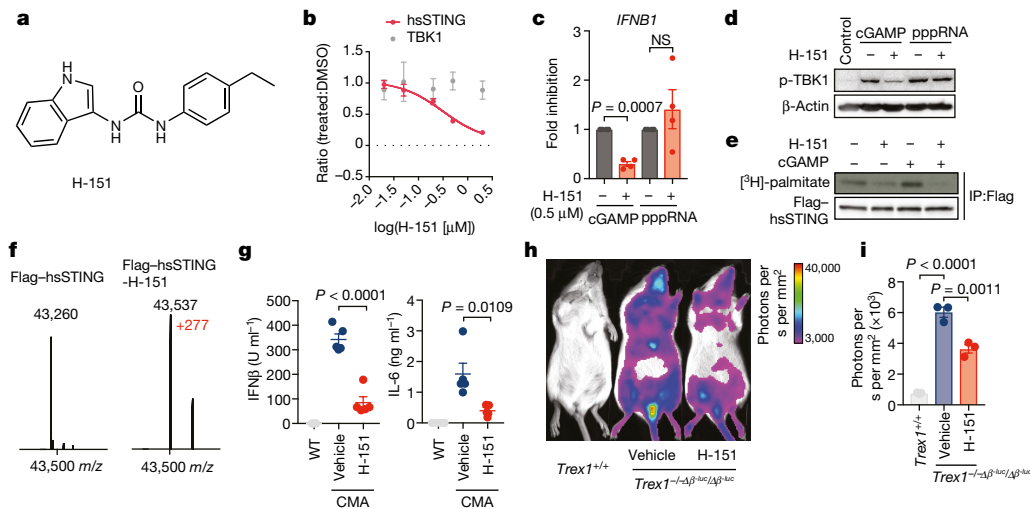


Fig. 5 | H-151 is a covalent STING antagonist. **a**, Structure of H-151. **b**, IFN β luciferase reporter measurements of HEK293T cells transfected as indicated (concentration of H-151 0.02–2 μ M). **c**, IFN β 1 mRNA levels in THP-1 cells pretreated with H-151 and stimulated as shown ($n = 4$). **d**, Immunoblots of p-TBK1 and β -actin of THP-1 cells stimulated for 2 h (H-151 0.5 μ M). **e**, [3 H]-palmitate incorporation of Flag-hsSTING after stimulation with cGAMP (3 h) (H-151, 1 μ M). **f**, Deconvoluted electrospray ionization mass spectra for Flag-hsSTING purified from treated cells as indicated. **g**, Serum levels of type I IFNs and IL-6 from

H-151 (H-151-AL), we observed a concentration-dependent interaction with hsSTING, with low background reactivity (Extended Data Fig. 9d–g). Mass spectrometry analysis of hsSTING purified from cells treated with H-151 revealed a mass shift that can be explained by an irreversible addition of H-151 to hsSTING (Fig. 5f). Mutagenesis studies together with top-down LC-MS/MS analysis confirmed that the irreversible modification introduced by H-151 to hsSTING again depended on Cys91 (Extended Data Fig. 9h–j and Supplementary Information). We next investigated the bioactivity of the H-151 compound in mice (Extended Data Fig. 10a, b). After intraperitoneal administration, H-151 reached effective systemic levels, displayed a short half-life in the serum and formed an adduct to mmSTING (Extended Data Fig. 10c, d). Notably, pretreatment of H-151 markedly reduced systemic cytokine responses in CMA-treated mice (Fig. 5g). Moreover, H-151 exhibited notable efficacy in *Trex1*^{-/-} mice that expressed a bioluminescent IFN β reporter, when administered for one week (Fig. 5h, i). Taken together, these data show that H-151 is a highly potent and selective small-molecule antagonist of STING that has noteworthy inhibitory activity both in human cells and in vivo.

In summary, we report the discovery of small-molecule inhibitors of STING that exploit an unanticipated covalent mechanism of action (Extended Data Fig. 11). Moreover, our study provides proof-of-concept that STING antagonists are efficacious in the treatment of autoinflammatory disease. The possibility of being able to pharmacologically antagonize STING may advance our understanding of its relevance in various contexts of health and disease.

Online content

Any Methods, including any statements of data availability and Nature Research reporting summaries, along with any additional references and Source Data files, are available in the online version of the paper at <https://doi.org/10.1038/s41586-018-0287-8>.

Received: 8 September 2017; Accepted: 24 May 2018;
Published online 4 July 2018.

- Ishikawa, H., Ma, Z. & Barber, G. N. STING regulates intracellular DNA-mediated, type I interferon-dependent innate immunity. *Nature* **461**, 788–792 (2009).
- Sun, L., Wu, J., Du, F., Chen, X. & Chen, Z. J. Cyclic GMP–AMP synthase is a cytosolic DNA sensor that activates the type I interferon pathway. *Science* **339**, 786–791 (2013).

wild-type mice treated with H-151 and stimulated with CMA ($n = 5$) or controls ($n = 3$). **h**, Representative luciferase activity measurement of *Trex1*^{-/-} *Irfn1* $\Delta\beta$ -*luc*/ $\Delta\beta$ -*luc* mice treated with H-151 or vehicle (each group, $n = 3$ mice) for 7 days. Wild-type reporter mice served as control ($n = 3$). **i**, Luciferase whole body integration. Data are mean \pm s.e.m. (**b**, **c**, **g**, **i**). NS, not significant. *P* values calculated using two-tailed *t*-test (**c**) or one-way ANOVA (**g**, **i**). For gel source data, see Supplementary Fig. 1. For source data, see Supplementary Table 1.

- Burdette, D. L. et al. STING is a direct innate immune sensor of cyclic di-GMP. *Nature* **478**, 515–518 (2011).
- Ablasser, A. et al. cGAS produces a 2'-5'-linked cyclic dinucleotide second messenger that activates STING. *Nature* **498**, 380–384 (2013).
- Diner, E. J. et al. The innate immune DNA sensor cGAS produces a noncanonical cyclic dinucleotide that activates human STING. *Cell Reports* **3**, 1355–1361 (2013).
- Gao, P. et al. Cyclic [G(2',5')pA(3',5')p] is the metazoan second messenger produced by DNA-activated cyclic GMP–AMP synthase. *Cell* **153**, 1094–1107 (2013).
- Wu, J. et al. Cyclic GMP–AMP is an endogenous second messenger in innate immune signaling by cytosolic DNA. *Science* **339**, 826–830 (2013).
- Zhang, X. et al. Cyclic GMP–AMP containing mixed phosphodiester linkages is an endogenous high-affinity ligand for STING. *Mol. Cell* **51**, 226–235 (2013).
- Abe, T. & Barber, G. N. Cytosolic-DNA-mediated, STING-dependent proinflammatory gene induction necessitates canonical NF- κ B activation through TBK1. *J. Virol.* **88**, 5328–5341 (2014).
- Barber, G. N. STING: infection, inflammation and cancer. *Nat. Rev. Immunol.* **15**, 760–770 (2015).
- Gall, A. et al. Autoimmunity initiates in nonhematopoietic cells and progresses via lymphocytes in an interferon-dependent autoimmune disease. *Immunity* **36**, 120–131 (2012).
- Jeremiah, N. et al. Inherited STING-activating mutation underlies a familial inflammatory syndrome with lupus-like manifestations. *J. Clin. Invest.* **124**, 5516–5520 (2014).
- Liu, Y. et al. Activated STING in a vascular and pulmonary syndrome. *N. Engl. J. Med.* **371**, 507–518 (2014).
- Crow, Y. J. & Manel, N. Aicardi–Goutières syndrome and the type I interferonopathies. *Nat. Rev. Immunol.* **15**, 429–440 (2015).
- Ahn, J., Gutman, D., Saijo, S. & Barber, G. N. STING manifests self DNA-dependent inflammatory disease. *Proc. Natl Acad. Sci. USA* **109**, 19386–19391 (2012).
- Ahn, J. et al. Inflammation-driven carcinogenesis is mediated through STING. *Nat. Commun.* **5**, 5166 (2014).
- An, J. et al. Expression of cyclic GMP–AMP synthase in patients with systemic lupus erythematosus. *Arthritis Rheumatol.* **69**, 800–807 (2017).
- King, K. R. et al. Irf3 and type I interferons fuel a fatal response to myocardial infarction. *Nat. Med.* **23**, 1481–1487 (2017).
- Zeng, L. et al. ALK is a therapeutic target for lethal sepsis. *Sci. Transl. Med.* **9**, eaan5689 (2017).
- Kerur, N. et al. cGAS drives noncanonical-inflammasome activation in age-related macular degeneration. *Nat. Med.* **24**, 50–61 (2018).
- Cavlar, T., Deimling, T., Ablasser, A., Hopfner, K. P. & Hornung, V. Species-specific detection of the antiviral small-molecule compound CMA by STING. *EMBO J.* **32**, 1440–1450 (2013).
- Conlon, J. et al. Mouse, but not human STING, binds and signals in response to the vascular disrupting agent 5,6-dimethylxanthenone-4-acetic acid. *J. Immunol.* **190**, 5216–5225 (2013).
- Dennehy, M. K., Richards, K. A., Wernke, G. R., Shyr, Y. & Liebler, D. C. Cytosolic and nuclear protein targets of thiol-reactive electrophiles. *Chem. Res. Toxicol.* **19**, 20–29 (2006).

24. Weerapana, E. et al. Quantitative reactivity profiling predicts functional cysteines in proteomes. *Nature* **468**, 790–795 (2010).
25. Saitoh, T. et al. Atg9a controls dsDNA-driven dynamic translocation of STING and the innate immune response. *Proc. Natl Acad. Sci. USA* **106**, 20842–20846 (2009).
26. Mukai, K. et al. Activation of STING requires palmitoylation at the Golgi. *Nat. Commun.* **7**, 11932 (2016).
27. Stetson, D. B., Ko, J. S., Heidmann, T. & Medzhitov, R. Trex1 prevents cell-intrinsic initiation of autoimmunity. *Cell* **134**, 587–598 (2008).
28. Gao, D. et al. Activation of cyclic GMP–AMP synthase by self-DNA causes autoimmune diseases. *Proc. Natl Acad. Sci. USA* **112**, E5699–E5705 (2015).
29. Gray, E. E., Treuting, P. M., Woodward, J. J. & Stetson, D. B. Cutting edge: cGAS is required for lethal autoimmune disease in the Trex1-deficient mouse model of Aicardi–Goutières Syndrome. *J. Immunol.* **195**, 1939–1943 (2015).

Acknowledgements We thank N. Jordan, E. Simeoni and L. Muhandes for technical assistance and advice. We acknowledge the staff of the BSF-ACCESS screening platform at the EPFL for support, especially M. Chambon and J. Bortoli, and the staff of the ISIC Mass Spectrometry platform at the EPFL, especially N. Gasilova. We thank the following core facilities for their support: BIoP, CPG and HCF. A.A. received grants from the SNF (BSSGIO-155984, 31003A_159836), the Gebert R uf Foundation (GRS-059_14) and the Else Kr oner-Fresenius Stiftung (2014_A250). R.B. received funding from an AGS Research Award and the German Research council (DFG - BE 5877/2-1).

Reviewer information *Nature* thanks Z. Chen, T. Taguchi, H. Wu and the other anonymous reviewer(s) for their contribution to the peer review of this work.

Author contributions S.M.H., M.F.G., L.R., L.A., A.D. and M.H. designed, performed and analysed experiments, and S.M.H. and M.F.G. assisted in writing the manuscript. L.R. and A.G. synthesized chemical compounds. R.B. and M.F.G. designed, performed and analysed animal experiments. G.T. and G.F.v.d.G. provided advice. A.A. designed, performed and analysed experiments, wrote the manuscript with input from all authors, conceived the idea and supervised the study.

Competing interests A.A. is a consultant to IFM Therapeutics, LLC. A.A., S.M.H., L.R. and the EPFL have filed provisional patent applications related to STING inhibitors. All other authors declare no competing interests.

Additional information

Extended data is available for this paper at <https://doi.org/10.1038/s41586-018-0287-8>.

Supplementary information is available for this paper at <https://doi.org/10.1038/s41586-018-0287-8>.

Reprints and permissions information is available at <http://www.nature.com/reprints>.

Correspondence and requests for materials should be addressed to A.A.

Publisher's note: Springer Nature remains neutral with regard to jurisdictional claims in published maps and institutional affiliations.

METHODS

Cells and cell culture conditions. Cells were cultured under 5% CO₂ and ambient O₂ at 37 °C in DMEM containing 10% fetal bovine serum (FBS), 100 IU ml⁻¹ penicillin and 100 µg ml⁻¹ streptomycin. BMDMs were generated by culturing bone marrow cells from wild-type mice in L929-conditioned medium. Mouse embryonic fibroblasts were generated according to standard conditions. LL171 cells and their use have previously been described³⁰. WI-38 cells and were purchased from ATCC. THP-1 cells were provided by A. Rösen-Wolff (University Hospital Dresden) and cultured in RPMI-1640 containing 10% FBS, 100 IU ml⁻¹ penicillin and 100 µg ml⁻¹ streptomycin. HEK293T cells were from D. Trono (EPFL). Cell lines were repeatedly tested for mycoplasma by PCR. No method of cell line authentication was used.

Mice and in vivo studies. C57BL/6J mice (stock number 000664) were purchased from Jackson Laboratories. TREX1-deficient mice were a gift from T. Lindahl³¹ and were backcrossed for > 10 generations to C57BL/6NJ. Mice were maintained under specific-pathogen-free (SPF) conditions at EPFL. For the pharmacokinetic studies, wild-type mice were injected intraperitoneally with 750 nmol C-176 per mouse in 200 µl corn oil (Sigma). Blood was collected at 30 min, 2 h and 4 h and serum C-176 levels were measured by mass spectrometry (liquid chromatography-high-resolution mass spectrometry). To assess the in vivo inhibitory effect of C-176, wild-type mice (8–12 weeks of age) were injected either with vehicle or C-176. After 1 h or 4 h, CMA was administered at a concentration of 224 mg kg⁻¹. Four hours later, mice were euthanized and the serum was collected to measure CMA-induced cytokine levels. To assess the in vivo inhibitory effect of H-151, wild-type mice were injected intraperitoneally with 750 nmol H-151 per mouse in 200 µl 10% Tween-80 in PBS. After 1 h CMA (112 mg kg⁻¹) was administered, and after 4 h mice were euthanized and the serum was collected. The efficacy study in *Trex1*^{-/-} mice was conducted as follows: mice (2–5 weeks of age) were injected with 7.5 µl of C-176 or DMSO dissolved in 85 µl corn oil twice per day for 11 consecutive days. Mice were euthanized by anaesthetization in a CO₂ chamber followed by cervical dislocation. For toxicology studies, 8-week-old mice were injected daily with 562.5 nmol of C-176 for 2 weeks. At day 14, blood samples were collected in lithium-heparin-coated tubes (Microvette CB 300 Hep-Lithium), and plasma was isolated after centrifugation at 4 °C and then stored at -80 °C. Plasma parameters were measured using DimensionXpand Plus (Siemens Healthcare Diagnostics AG). For the peripheral blood cell profile, 100 µl of blood was collected in EDTA-K-coated tubes (Microvette CB 300 EDTA K2). Complete blood counts were analysed with an ADVIA120 haematology system (Siemens Healthcare Diagnostics AG). For the detection of luciferase activity, *Trex1*^{-/-}*Irfn1*^{Δβ-luc/Δβ-luc} reporter mice³² (aged 4–7 weeks) were injected intraperitoneally daily for 7 days with 750 nmol H-151 or DMSO in 200 µl PBS 0.1% Tween-80. For in vivo imaging, mice were anaesthetized with isoflurane and injected intravenously with 15 mg kg⁻¹ Xenolight D-luciferin (Perkin Elmer) in isotonic sodium chloride. Photon flux was quantified two minutes after injection on an In-vivo Xtreme II imaging device (Bruker) with binning set to 8 × 8 pixels and an integration time of 3 min. Animal experiments were approved either by the Service de la Consommation et des Affaires Vétérinaires of the canton of Vaud (Switzerland) or by the Landesdirektion Dresden (Germany) and were performed in accordance with the respective legal regulations.

Cell-based IFNβ promoter-reporter luciferase measurements. HEK293T cells were seeded in a 96-well plate and transfected using GeneJuice (Millipore) with a IFN-β promoter-reporter plasmid (pIFNβ-GLuc) in combination with indicated expression constructs. After 16 h, gaussian luciferase activity was measured in the supernatants using coelenterazine (PJK GmbH) as substrate.

High-throughput chemical compound screen. HEK293T cells that expressed mouse STING with an N-terminal mCherry tag³⁰ were transfected using GeneJuice (Millipore) with a construct encoding for cyclic di-GMP synthase in conjunction with an IFN-β firefly luciferase reporter plasmid. Three hours later, transfected cells were seeded in 384-well plates (Corning) coated with library compounds. For each compound, a 40-µl volume was selected to obtain a concentration of 10 µM in the assay plates. The amount of DMSO in each well was normalized to 0.1%. After overnight treatment, cells were lysed in lysis buffer (25 mM Tris-phosphate (pH 7.8), 2 mM DTT, 2 mM 1,2-diaminocyclohexane-N,N,N',N'-tetraacetic acid, 10% glycerol, 1% Triton X-100) for 20 min followed by the addition of firefly luciferase substrate. Reporter activity was measured using a Tecan Infinite plate reader. The screen was performed on ~20,000 compounds from a chemically diverse compound collection available at the BSF core facility at EPFL. For the identification of hsSTING-specific compounds, HEK293T cells expressing a human STING construct were transfected with a construct encoding mouse cyclic GMP-AMP synthase in conjunction with an IFN-β firefly luciferase reporter plasmid. Further analysis was performed as described above. The screen was performed on ~30,000 compounds from a chemically diverse compound collection available at the BSF core facility at EPFL.

Histological analyses. Tissues were fixed in 4% formaldehyde solution (SAV LP), embedded in paraffin, and sections were stained with haematoxylin (Merck) and eosin (Shandon) (H & E). Five individual sections of the same heart were scored for levels of tissue damage (0–3) and inflammation (0–3). Scores represent the sum per organ.

Type I IFN bioassay and enzyme-linked immunosorbent assay. Levels of mouse type I IFN were determined by incubating LL171 cells that stably express an ISRE-luciferase construct with supernatants or serum for 5 h. LL171 cells were lysed in passive lysis buffer (Promega) and luciferase activity was measured using luciferin as substrate. Levels of mouse IL-6 and human IP-10 were determined by enzyme-linked immunosorbent assay (BD Bioscience) according to the manufacturer's instructions.

Stimulation of cells. BMDMs (1 × 10⁶ cells ml⁻¹) were pretreated with DMSO, C-178 (0.5 µM unless otherwise indicated) or H-151 (0.5 µM) for 1 h, followed by stimulation with either CMA (250 µg ml⁻¹, Sigma), dsDNA (90-mer, 1.33 µg ml⁻¹), cyclic di-GMP or cGAMP (1.5 µg ml⁻¹, Biolog). Triphosphate RNA (166 ng ml⁻¹) or LPS (1 µg ml⁻¹, Invivogen) were used as controls. THP-1 cells (1 × 10⁶ cells ml⁻¹) were differentiated with PMA (100 ng ml⁻¹, Sigma) for at least 3 h and treated with C-170 (0.5 µM) or H-151 (0.5 µM or as indicated) for 2 h, followed by stimulation with cyclic GAMP (375 ng ml⁻¹) or triphosphate RNA (133 ng ml⁻¹) for 2–3 h (for mRNA expression analysis and p-TBK1 immunoblot) or overnight (for IP-10 production). Alternatively, WI-38 cells (0.15 × 10⁶ cells ml⁻¹) and THP-1 (1 × 10⁶ cells ml⁻¹) cells were pretreated with C-178 (0.5 µM) and stimulated with cGAMP (1.5 µg ml⁻¹) for 2–3 h. To transfect dsDNA, triphosphate RNA and cyclic dinucleotides, Lipofectamine 2000 (Life Technologies) was used. The sequence of the sense strand of the 90-mer DNA is as follows: 5'-TACAGATCTACTAGTGATCTATGACTGATCTGTACATGATCTACATACAGATCTACTAGTGATCTATGACTGATCTGTACATGATCTACA-3'.

Mutagenesis PCR and alanine scanning. Point mutants were generated by site-directed PCR mutagenesis via the Quikchange Primer Design method (Agilent) using PrimeSTAR Max DNA Polymerase (Takara) and suitable primers. Alanine scanning was performed as follows: HEK293T cells were plated in 96-well plates, transfected with plasmids encoding individual mmSTING alanine point-mutants together with an IFN-β luciferase reporter using GeneJuice (Merck Millipore), and then treated with C-178. Luciferase activity was assessed after overnight incubation and normalized to values obtained for wild-type mmSTING.

RNA sequencing. BMDMs were pretreated with C-178 for 1 h, followed by 2 h of stimulation with either DMSO or CMA. After CMA stimulation, RNA was isolated using RNeasy Mini kit (Qiagen). mRNA sequencing libraries were prepared using the TruSeq mRNA stranded LT (Illumina) kit. Samples were sequenced by the NextSeq 500 system sequencing with 1 × 75 cycle ('single read'), 'high output' mode. Resultant data files were converted to fastq format, demultiplexed into constituent libraries and trimmed. Short reads were aligned to the mouse genome mm10. Library preparation, RNA sequencing and differential gene expression analysis was performed by Microsynth (Switzerland). Heat maps of normalized values were generated using the web-based platform Automated Single-cell Analysis Pipeline³³.

Western blot analysis. Cells were lysed in 2 × Laemmli buffer, immobilized protein on beads in sample reducing buffer followed by denaturing at 95 °C for 5 min. Cell lysates were separated by SDS-PAGE and transferred onto PVDF membranes. Blots were incubated with anti-STING (D2P2F), phospho-TBK1 (D52C2), TBK1 (D1B4) (all Cell Signaling Technology), anti-transferrin receptor (Thermo Scientific, 136800) anti-calnexin (Millipore, MAB3126) or anti-Flag M2 (Sigma, F3165). As secondary antibodies, anti-rabbit-IgG-HRP or anti-mouse-IgG-HRP (1:2000) (Santa Cruz Biotechnology) were used. Anti-β-actin (C4, Santa Cruz, 1:5000) was used as control. ECL signal was recorded on the ChemiDoc XRS Biorad Imager and data were analysed with Image Laboratory (Biorad).

Quantitative RT-qPCR. Total RNA was isolated using the RNeasy Mini Kit (Qiagen) and cDNA was synthesized using the RevertAid First Strand cDNA Synthesis kit (Fermentas). Quantitative RT-qPCR was performed in duplicates using Maxima SYBR Green Master Mix (Thermo Scientific) on a QuantStudio 5 machine. GAPDH was used as an endogenous normalization control to obtain relative expression data. Primer sequences are as follows: mmGapdh forward, 5'-GTCATCCCAGAGCTGAACG-3'; mmGapdh reverse, 5'-TCATACTTGGCAGGTTTCTCC-3'; mmIrfn1 forward, 5'-CTCCA GCTCCAAGAAAGGAC-3'; mmIrfn1 reverse, 5'-TGGCAAAGGCAGTGAAC TC-3'; mmTnf forward, 5'-TATGGCCAGACCCTCACA-3'; mmTnf reverse, 5'-GGAGTAGACAAGGTACAACCCATC-3'; mmIsg15 forward, 5'-AAGAAGC AGATTGCCAGAA-3'; mmIsg15 reverse, 5'-TCTGCGTCAGAAAGACCTCA-3'; mmCxcl10 forward, 5'-AAGTGTGCTCCGTCATTTCT-3'; mmCxcl10 reverse, 5'-GTGGCAATGATCTCAACAG-3'; hsGAPDH forward, 5'-GAGTCAACG GATTGTGTCGT-3'; hsGAPDH reverse, 5'-GACAAGCTTCCCCTTCTCAG-3'; hsIFNB1 forward, 5'-CAGCATCTGCTGGTTGAAGA-3'; hsIFNB1 reverse,

5'-CATTACCTGAAGGCCAAGGA-3'; hsTNF forward, 5'-CCCAGT GACAAGCCTGTAG-3'; hsTNF reverse, 5'-TGAGGTACAGGCCCTCTGAT-3'.

Metabolic labelling with [³H]-palmitate. Indicated Flag–STING constructs were expressed in HEK293T cells. For metabolic labelling, cells were starved for 1 h in Glasgow minimal essential medium buffered with 10 mM Hepes, pH 7.4 with C-178 or C-176 (1 μM). Cells were then incubated for 2 h in IM with 200 μCi ml⁻¹ [³H]-palmitic acid (9,10-³H(N)) (American Radiolabelled Chemicals) in presence of C-178 or C-176, and with or without stimulation with CMA (250 μg ml⁻¹). For immunoprecipitation, cells were washed three times in PBS, lysed for 30 min at 4 °C in the following buffer (0.5% Nonidet P-40, 500 mM Tris pH 7.4, 20 mM EDTA, 10 mM NaF, 2 mM benzamidein and protease inhibitor cocktail (Roche)) and centrifuged for 3 min at 5000 r.p.m. Supernatants were incubated overnight at 4 °C with the appropriate antibodies (anti-Flag, anti-transferrin receptor and anti-calnexin) and G sepharose beads (GE Healthcare, 17-0618-01). For radiolabelling experiments, after immunoprecipitation washed beads were incubated for 5 min at 90 °C in reducing sample buffer before 4–20%-gradient SDS–PAGE. Following SDS–PAGE, gels were incubated in a fixative solution (25% isopropanol, 65% H₂O, 10% acetic acid) and incubated for 30 min with signal enhancer Amplify NAMP100 (GE Healthcare). The radiolabelled products were revealed using autoradiography and quantified using the Typhoon Imager (ImageQuantTool, GE Healthcare).

Competition assay. HEK293T cells expressing Flag–STING were incubated with the indicated compounds and after 1 h, C-176-AL was added for 1 h. Cells were collected in PBS and analysed by in-gel analysis of C-176-AL-mediated labelling of STING (see 'Gel-based analysis of compound binding to STING').

Immunoprecipitation. Flag–STING expression was induced in HEK293T cells overnight by doxycycline (Sigma). Cells were incubated with or without C-178 or C-176 (1 μM) for 1 h and treated with DMSO or CMA (250 μg ml⁻¹) for 2 h. Cells were washed in PBS and lysed in lysis buffer (50 mM HEPES, 150 mM NaCl, 10% glycerin, 1 mM MgCl₂, 1 mM CaCl₂, 1% Brij-58 and protease inhibitor cocktail (Sigma P8340)) for 30 min. Flag–STING was immunoprecipitated using anti-Flag M2 affinity gel agarose gel (Sigma) for 2 h at 4 °C. After stringent washing in lysis buffer and PBS, the supernatant was completely removed and the resin was boiled in sample buffer before SDS–PAGE was performed. For immunoprecipitation of endogenous STING, splenocytes were lysed in the above-mentioned lysis buffer and incubated with anti-STING (RD System AF6516) and G sepharose beads (GE Healthcare, 17-0618-01) overnight. Beads were washed in PBS and gel-based analysis of C-176-AL binding to STING was performed.

Gel-based analysis of compound binding to STING. HEK293T cells expressing Flag–STING were incubated with C-176-AL, C-175-AZ, iodoacetamide azide (Thermo Fisher) or H-151-AL in serum-free medium, collected in PBS and lysed by repetitive freezing and thawing. Forty-three microlitres of lysed cells was treated with a freshly prepared 'click reagent' mixture containing tris(benzyltriazolylmethyl)amine (TBTA) (3 μl per sample, 3 mM in 1:4 DMSO:*t*-ButOH), tetramethylrhodamine (TAMRA) azide (Thermo Fisher), SiR azide (Spirochrome) or SiR alkyne (Spirochrome) (2 μl per sample, 1.25 mM in DMSO), and freshly prepared CuSO₄ (1 μl per sample) and tris-(2-carboxyethyl)phosphine hydrochloride (TCEP) (1 μl per sample) and incubated at room temperature for 30 min. The reaction was quenched by addition of reducing sample buffer. In-gel fluorescence was visualized using Fusion FX (Vilber Lourmat) and analysed by Fusion capt advance acquisition software.

Crosslinking with disuccinimidyl suberate. HEK293T cells expressing Flag–mmSTING were incubated with or without C-176 (1 μM) for 1 h and treated with DMSO or CMA (250 μg ml⁻¹) for 2 h. Crosslinking was performed in PBS with 1 mM disuccinimidyl suberate (DSS) (Thermo Fisher) freshly prepared in DMSO at room temperature for 1 h.

Blue native gel assay. Flag–STING expression was induced in HEK293T cells overnight by doxycycline. Cells were washed, collected and lysed using the native PAGE sample preparation kit (Invitrogen) in 1% digitonin according to the manufacturer's instructions. Lysates were run on native PAGE 4–16%-Bis-Tris gel and transferred on a PVDF membrane (Invitrogen).

Lentiviral vector production and transduction. HEK293T cells were transfected with pCMVDR8.74 and pMD2.G plasmids, and with the puromycin-selectable lentiviral vector pTRIPZ that contained the open reading frame of respective Flag–mmSTING or Flag–hsSTING constructs, using the calcium phosphate precipitation method. The supernatant that contained lentiviral particles was collected at 48 h and 72 h, pooled and then concentrated by ultracentrifugation. Wild-type mouse embryonic fibroblasts and HEK293T cells were transduced with the lentiviral vectors by adding 5 μl of concentrated stock directly to the culture medium.

Immunostaining. Mouse embryonic fibroblasts expressing Flag–mmSTING were seeded on coverslips, fixed with 2% (v/v) paraformaldehyde for 10 min, permeabilized for 5 min in 0.1% (v/v) Triton X-100 and blocked with 2% BSA in PBS for 20 min at room temperature. Samples were incubated with the primary antibodies for 3 h (anti-Flag M2 (F1804, Sigma) and GM130 (clone 35, BD Pharmingen,

Alexa Fluor 647). After washing, samples were incubated with secondary antibody (donkey anti-mouse Alexa Fluor 568 (Thermo Fisher)) containing 5 μg 6-diamino-2-phenylindole (DAPI) for 1 h at room temperature. Coverslips were mounted with Dak (fluorescent mounting medium). Images were acquired by a wide-field fluorescence microscope (Zeiss Axioplan) and processed in ImageJ software. Confocal sections were obtained with a confocal laser scanning microscope (Zeiss LSM710).

Intact mass measurements for mmSTING. Expression of Flag–mmSTING or Flag–mmSTING(C91S) expression was induced in HEK293T cells overnight by doxycycline. Cells were treated with or without C-178 or C-176 (1 μM) for 30 min and lysed in lysis buffer (20 mM Hepes, 150 mM NaCl, 10% glycerin and 1% DDM). Flag–STING was immunoprecipitated using anti-Flag M2 affinity gel agarose gel (Sigma) for 2 h at 4 °C. Precipitated proteins were eluted using the Flag peptide according to the manufacturer's instructions. Protein mass spectrometry was performed on a Shimadzu MS2020 connected to a Nexerra UHPLC system, equipped with a Waters ACQUITY UPLC BEH C4 1.7-μm, 2.1 × 50-mm column. Buffer A was 0.05% formic acid in water, and buffer B was 0.05% formic acid in acetonitrile. The analytical gradient was from 10% to 90% buffer B within 6.0 min with 0.75 ml min⁻¹ flow. Mass spectra were collected from 300–2,000 Da and the spectra were deconvoluted using the software MagTran.

Intact mass measurements for hsSTING and top-down analysis using LC-MS/MS. Proteins were prepared as described in 'Intact mass measurements for mmSTING'. For both intact mass measurement (LC-MS) and top-down analysis (liquid chromatography with high-energy collisional-induced dissociation tandem mass spectrometry, LC-HCD-MS/MS), samples were separated onto column Acquity UPLC Protein BEH C4 (300 Å, 1.7 μm, 1 × 150 mm, Waters) using a Dionex Ultimate 3000 analytical RSLC system (Dionex) coupled to a HESI source (Thermo Fisher Scientific). The separation was performed with a flow rate of 90 μl min⁻¹ by applying a gradient of solvent B from 15 to 45% in 2 min, then from 45 to 60% within 10 min, followed by column washing and re-equilibration steps. Solvent A was water with 0.1% formic acid, and solvent B was acetonitrile with 0.1% formic acid. Eluting proteoforms were analysed on a high-resolution QExactive HF-HT-Orbitrap-FT-MS benchtop instrument (Thermo Fisher Scientific). For intact mass measurements, MS1 scans were performed in protein mode with 15,000 resolution and averaging 10 micro-scans. Top-down analysis for localization of the compound binding site was performed in PRM mode, isolating specie at 947.5 and 941.6 *m/z*, with a 300-Th isolation window, 120,000 resolution and averaging 10 micro-scans. HCD was used as fragmentation method with normalized collision energy of 10%, 15% and 19%. Intact mass measurement data were analysed with Protein Deconvolution (Thermo Fisher Scientific) using Respect algorithm with 99% noise rejection confidence and 20 p.p.m. accuracy of average mass identification. Top-down data were deconvoluted using MASH Suite software (GE research group, University of Wisconsin). Data obtained with 3 different NCE values were combined together to create a fragmentation map with assigned *b*- and *y*-fragments using ProSight Lite software (Kelleher research group, Northwestern University) with 20 p.p.m. mass tolerance.

Chemical synthesis. All chemical reagents and anhydrous solvents for synthesis were purchased from commercial suppliers (Sigma-Aldrich, Fluka and Acros) and were used without further purification or distillation. C-176 and C-178 were either purchased (Vitas-M laboratory STK016322 and ChemBridge 5747493) or synthesized. The composition of mixed solvents is given by the volume ratio (v/v). ¹H and ¹³C nuclear magnetic resonance spectra were recorded on a Bruker DPX 400 (400 MHz for ¹H, 100 MHz for ¹³C, respectively) or Bruker AVANCE III 400 Nanobay (400 MHz for ¹H, 100 MHz for ¹³C, respectively) with chemical shifts (δ) reported in p.p.m. relative to the solvent residual signals of DMSO-d₆ (2.50 p.p.m. for ¹H, 39.52 p.p.m. for ¹³C). Coupling constants are reported in Hz. LC-MS was performed on a Shimadzu MS2020 connected to a Nexerra UHPLC system equipped with a Waters ACQUITY UPLC BEH C18 1.7-μm, 2.1 × 50-mm column. Buffer A was 0.05% HCOOH in H₂O, and buffer B was 0.05% HCOOH in acetonitrile. Analytical gradient was from 10% to 90% buffer B within 6.0 min with flow of 0.5 ml min⁻¹. For details of the chemical synthesis, see Supplementary Information.

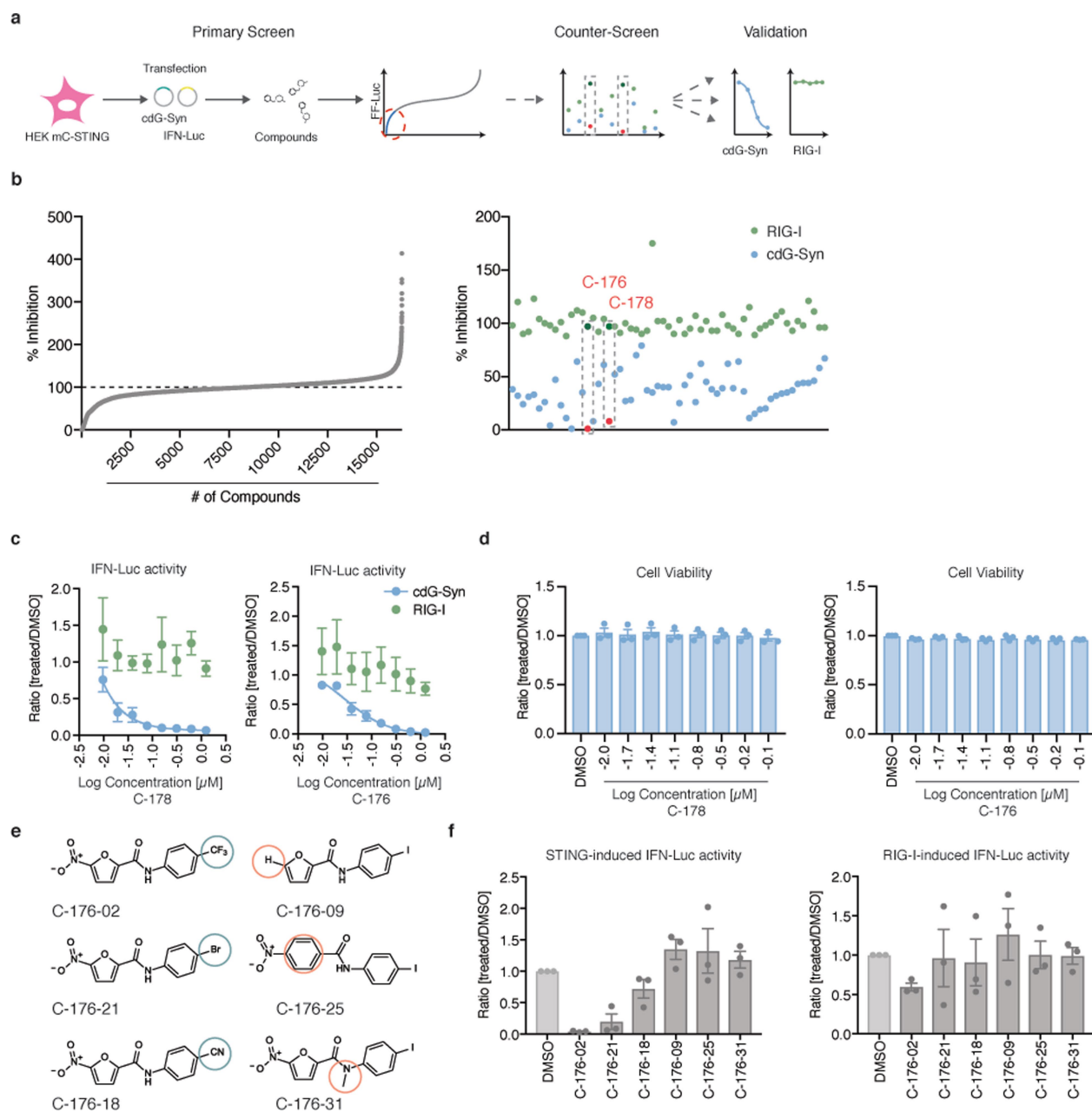
Statistical analysis. Prism software (Graphpad Software) was used to perform statistical tests and to generate graphs. Data are presented as mean ± s.e.m. or s.d. and *P* values were calculated as detailed in the corresponding legends. No statistical methods were used to predetermine sample sizes. Sample sizes were instead determined on the basis of previous experimental experience or based on general practices in the field. Replicates are biological replicates. For the in vivo studies, mice were randomly allocated to groups. For histological analysis of tissues, experimenters were blinded to the experimental conditions.

Reporting summary. Further information on experimental design is available in the Nature Research Reporting Summary linked to this paper.

Data availability. RNA sequencing data have been deposited in the Gene Expression Omnibus (GEO) under the accession code GSE113933. Full scans for

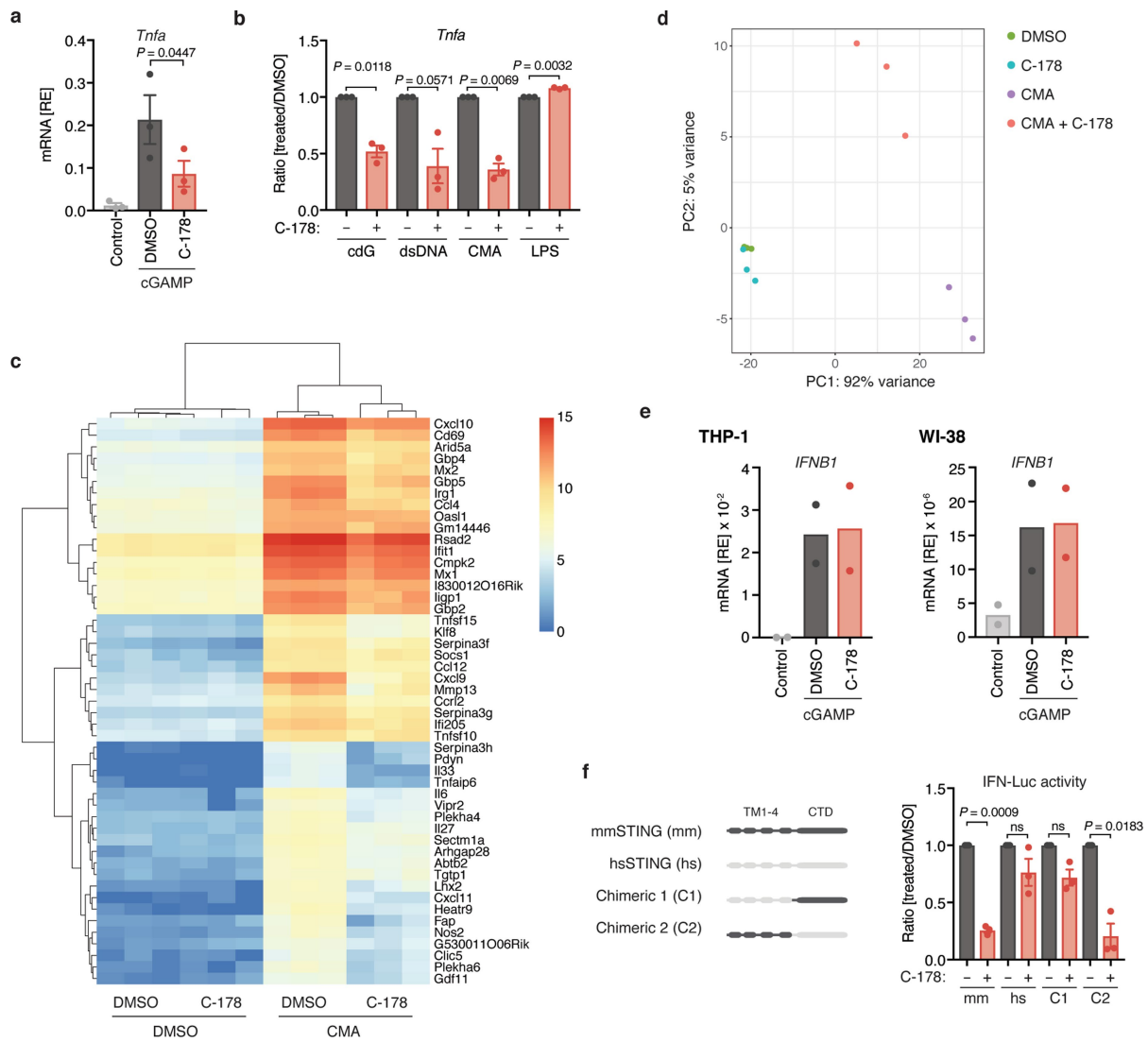
all western blots and in-gel fluorescence images are provided. Source Data for animal experiments from Figs 4, 5g–i and Extended Data Figs. 6b–g, 7b–d and 10c are shown in Supplementary Table 1. All other data are available from the corresponding author on reasonable request.

30. Ablasser, A. et al. Cell intrinsic immunity spreads to bystander cells via the intercellular transfer of cGAMP. *Nature* **503**, 530–534 (2013).
31. Morita, M. et al. Gene-targeted mice lacking the Trex1 (DNase III) 3'→5' DNA exonuclease develop inflammatory myocarditis. *Mol. Cell. Biol.* **24**, 6719–6727 (2004).
32. Peschke, K. et al. Loss of Trex1 in dendritic cells is sufficient to trigger systemic autoimmunity. *J. Immunol.* **197**, 2157–2166 (2016).
33. Gardeux, V., David, F. P. A., Shajkofci, A., Schwalie, P. C. & Deplancke, B. ASAP: a web-based platform for the analysis and interactive visualization of single-cell RNA-seq data. *Bioinformatics* **33**, 3123–3125 (2017).



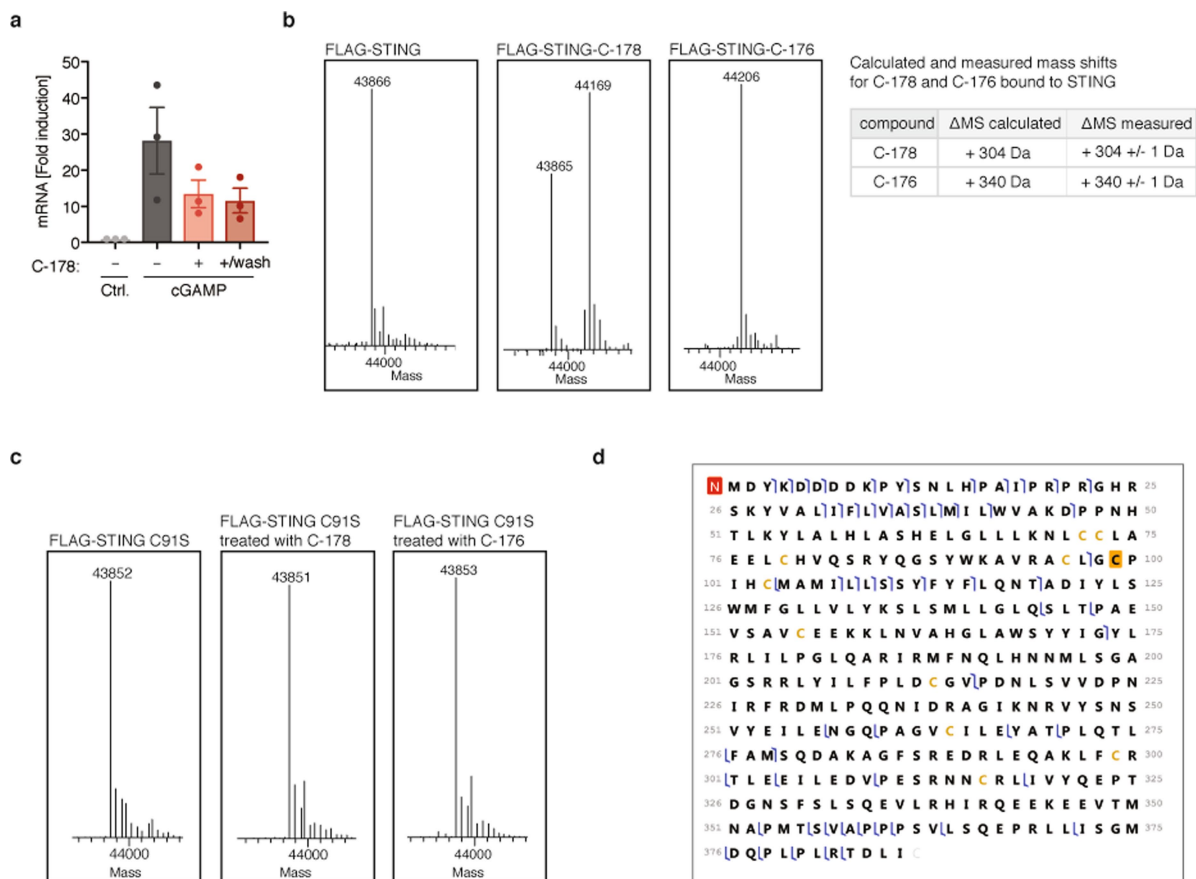
Extended Data Fig. 1 | A chemical screen identifies small-molecule inhibitors of STING. a, Screening workflow. HEK mC-STING, HEK293T cells expressing mCherry-STING. **b**, Left, summary of the primary screen. Mean of normalized values for IFN β luciferase activity in cells treated with compound versus cells treated with DMSO. Right, validation of selected candidates from the primary screen. Normalized values for IFN β luciferase activity (light blue) induced by coexpression of cyclic di-GMP synthase (cdG-Syn) and STING are shown, in comparison to activity triggered

by RIG-I (green). **c**, **d**, HEK293T cells expressing mCherry-STING were transfected with plasmids that encoded either cdG-Syn or RIG-I, as well as an IFN β luciferase reporter, and then treated with C-178 or C-176 (1.25 μ M–0.01 μ M), after which IFN β luciferase activity (**c**) or cell viability (using the CellTiter-Blue assay) (**d**) were measured. **e**, **f**, Chemical structures of derivatives of C-176 (**e**) and their effect (at a concentration of 0.5 μ M) on IFN β luciferase reporter activity triggered by mmSTING or RIG-I (**f**). Mean \pm s.e.m. of $n = 3$ experiments (**c**, **d**, **f**).



Extended Data Fig. 2 | Activity of C-178 against STING in distinct cells. **a, b**, mRNA expression levels of *Tnfa* in BMDMs activated with cGAMP, cyclic di-GMP (cdG), dsDNA, CMA or LPS for 5 h, after pretreatment for 1 h with C-178 (0.5 μ M) or DMSO ($n = 3$ biological replicates). **c**, Heat map of RNA sequencing analysis of BMDMs treated with DMSO or CMA, in the presence or absence of C-178. The top 50 upregulated genes in cells treated with DMSO versus cells treated with CMA, in the absence of C-178, are shown for all conditions. **d**, Scatter plot of the dimensions PC1 versus PC2. **e**, Levels of expression of *IFNB1* mRNA in

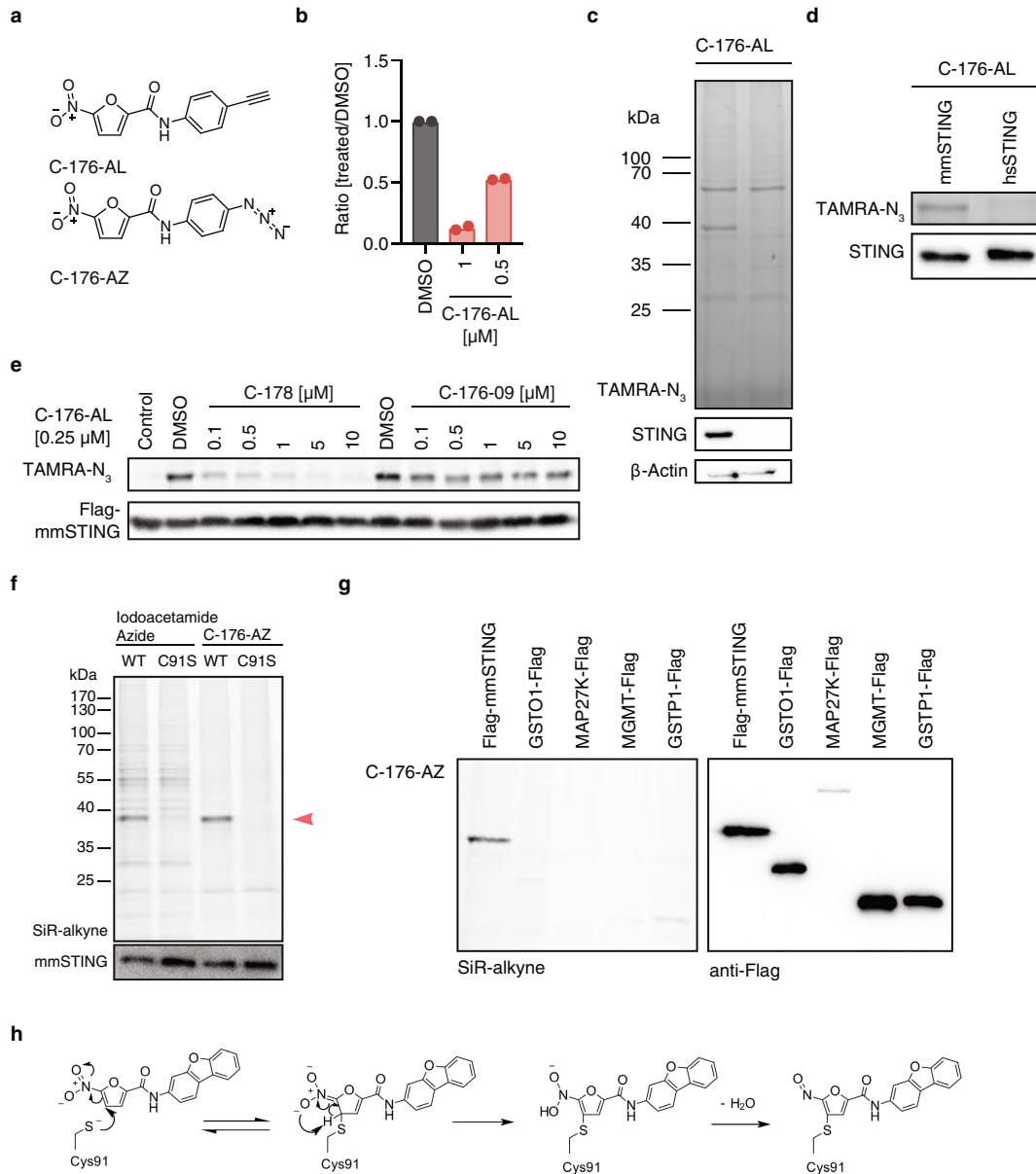
THP-1 and WI-38 cells pretreated with C-178 (0.25 μ M) or DMSO and stimulated with cGAMP for 3 h ($n = 2$ biological replicates). **f**, HEK293T cells were transfected with the construct chimaeric 1 (C1: hsSTING (amino acids 1–138)–mmSTING (amino acids 138–378)) or the construct chimaeric 2 (C2: mmSTING (amino acids 1–137)–hsSTING (amino acids 139–379)), together with cdG-Syn and IFN β luciferase reporter, and treated with C-178 (0.5 μ M) ($n = 3$ biological replicates). Data are mean or mean \pm s.e.m. P values were determined by two-tailed t -test.



Extended Data Fig. 3 | C-178 and C-176 covalently bind to Cys91.

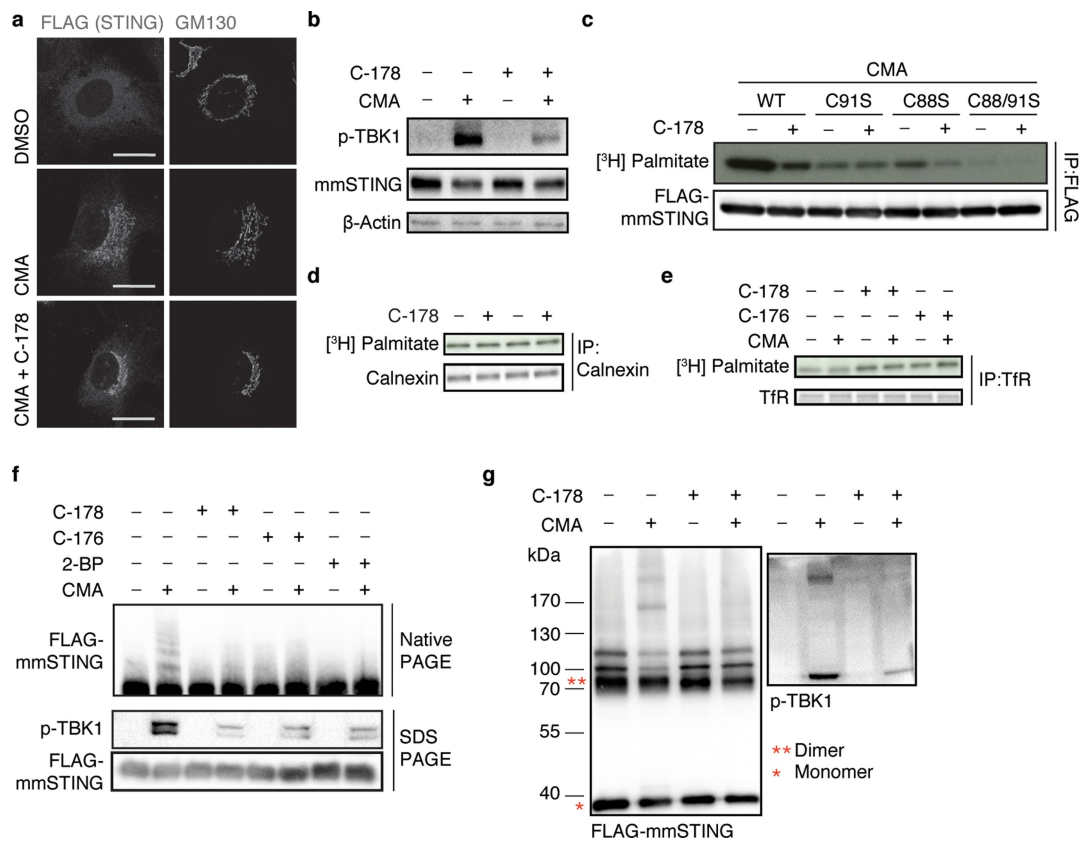
a, BMDMs were treated with C-178 (0.25 μ M) for 1 h, washed or left untreated and after 1 h were stimulated with cGAMP for 3 h. Levels of *Ifnb1* mRNA were assessed by RT-qPCR. Data are mean \pm s.e.m. ($n = 3$ biological replicates). **b–d**, HEK293T cells expressing indicated Flag-mmSTING constructs were exposed to C-178 or C-176 (1 μ M), lysed and Flag-mmSTING was immunoprecipitated. The eluted protein was analysed by intact mass spectrometry (LC-MS). **b**, Deconvoluted electrospray ionization mass spectrum (left), and expected and measured mass shifts after covalent binding of C-176 and C-178 (right) are shown.

c, Deconvoluted electrospray ionization mass spectrum for Flag-mmSTING(C91S). **d**, Fragmentation map of Flag-mmSTING-C-176 analysed by top-down analysis, using LC-HCD-MS/MS (an additional 8 residues are due to N-terminal Flag). Data that were obtained with three different NCE values are combined to create a fragmentation map with assigned *b*- and *y*-fragments. Achieved sequence coverage is 15% with 20 p.p.m. mass accuracy for fragment assignment. One representative of $n = 2$ independent experiments is shown (**b**, **c**). For electrospray ionization spectra see Supplementary Information.



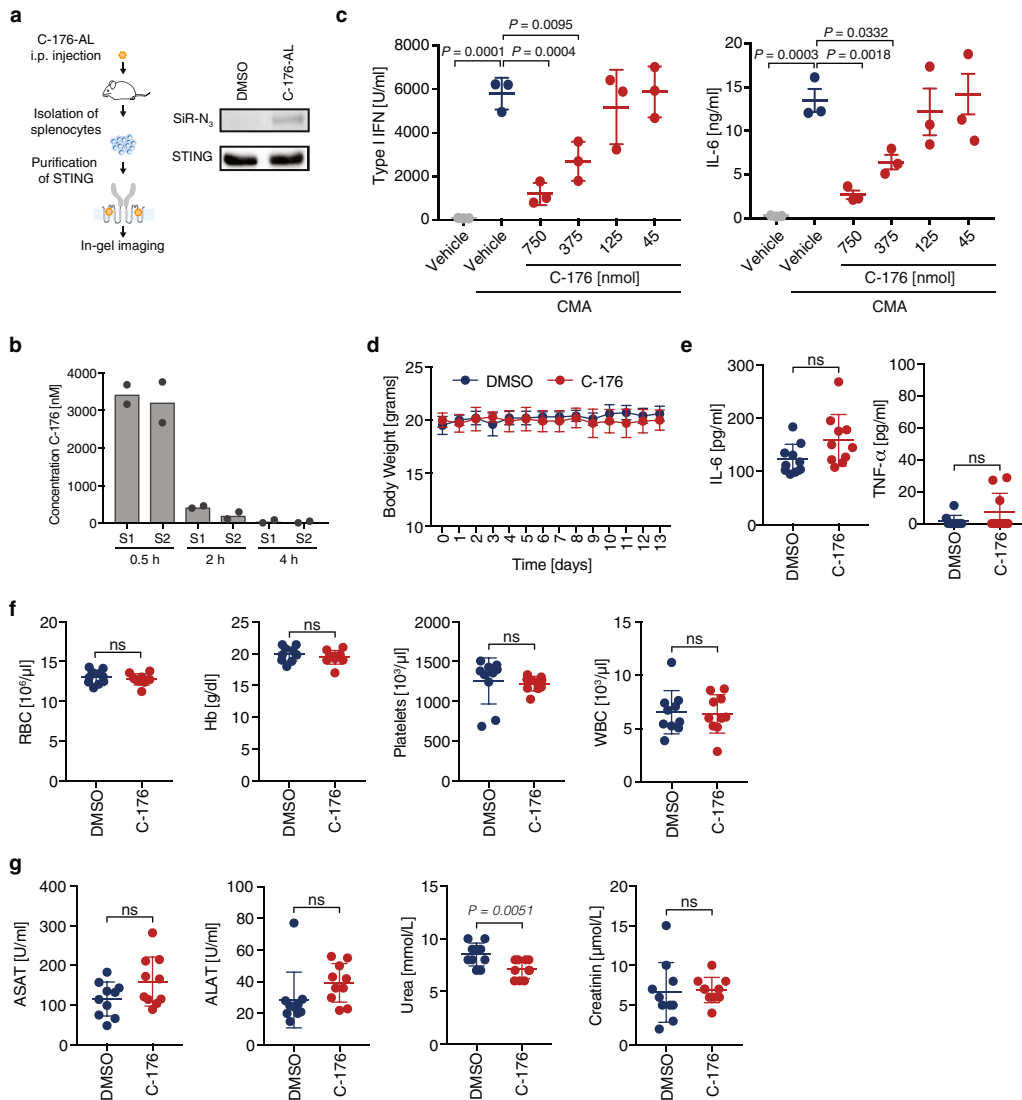
Extended Data Fig. 4 | Gel-based analysis of compound interactions using clickable probes. **a**, Structures of C-176-AL and C-176-AZ. **b**, HEK293T cells transfected with Flag-mmSTING and an IFN β luciferase reporter were treated with C-176-AL, and luciferase activity was then assessed. Data are mean of $n = 2$. **c**, Labelling events of wild-type HEK293T cells and HEK293T cells with Flag-mmSTING incubated with C-176-AL (0.25 μM). **d**, Distinct labelling of mmSTING and hsSTING by C-176-AL (0.25 μM). **e**, Concentration-dependent competitor blockage of C-176-AL (0.25 μM) against C-178 and C-176-09 in HEK293T cells that

express Flag-mmSTING. **f**, Labelling events of HEK293T cells that express Flag-mmSTING (wild-type mmSTING or mmSTING(C91S)) when exposed to iodoacetamide azide or C-176-AZ (both at 0.25 μM). **g**, HEK293T cells expressing Flag-mmSTING, GSTO1-Flag, MAP27K-Flag, MGMT-Flag or GSTP1-Flag were treated with C-176-AZ (0.25 μM). For in-gel fluorescence imaging, TAMRA azide (**c-e**) or SiR alkyne (**f, g**) was used. Immunoblots against Flag or β -actin are shown and data are representative of $n = 3$ independent experiments (**c-g**). **h**, Proposed reaction mechanism. For gel source data, see Supplementary Fig. 1.



Extended Data Fig. 5 | C-178 and C-176 block activation-induced palmitoylation of STING. **a**, Single-channel images of Flag and GM130 stainings of mouse embryonic fibroblasts that express Flag-mmSTING (control corresponding to images shown in Fig. 3), treated with CMA or DMSO. Scale bar, 20 μ m. **b**, Protein quantification of p-TBK1, Flag-mmSTING and β -actin by immunoblot of mouse embryonic fibroblasts from **a**. **c**, [³H]-palmitate labelling of HEK293T cells that express the indicated Flag-mmSTING constructs, and which were treated with C-178, C176 (1 μ M) or DMSO. **d**, **e**, [³H]-palmitate labelling of immunoprecipitated endogenous calnexin or transferrin receptor from

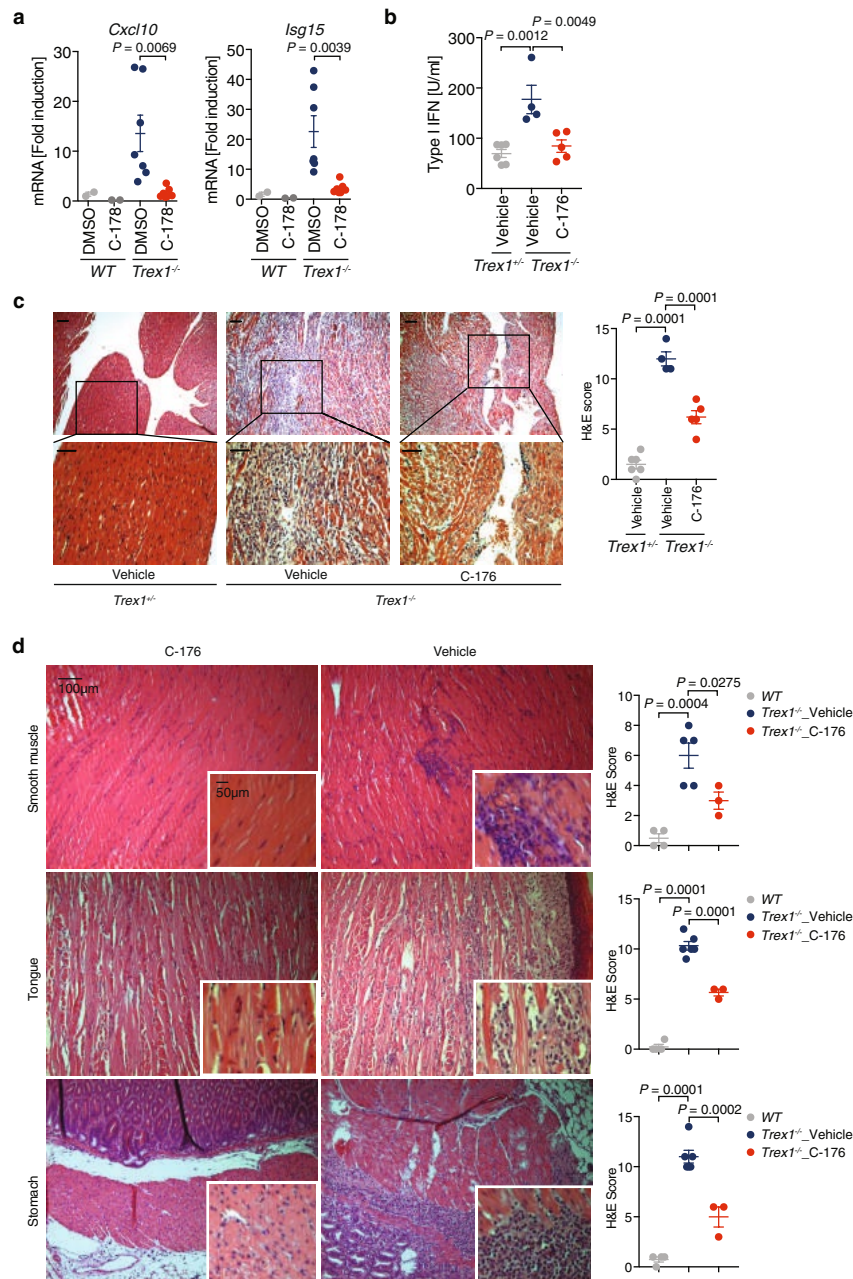
HEK293T cells treated as indicated (compounds at 1 μ M). **f**, HEK293T cells that express Flag-mmSTING were treated with C-178 (1 μ M) or 2-bromopalmitate (2-BP) (50 μ M) and stimulated with CMA for 1.5 h. Analysis of indicated proteins was performed by native PAGE or SDS-PAGE. **g**, Crosslinked lysates (DSS, 1 mM) of HEK293T cells that express Flag-mmSTING treated with C-178 (1 μ M) and stimulated with CMA (2 h) were analysed by SDS-PAGE and immunoblotted for STING and p-TBK1. One representative of $n = 3$ (**a-c**, **e-g**) or $n = 2$ (**d**) independent experiments. For gel source data, see Supplementary Fig. 1.



Extended Data Fig. 6 | In vivo effects of C-176 in wild-type mice.

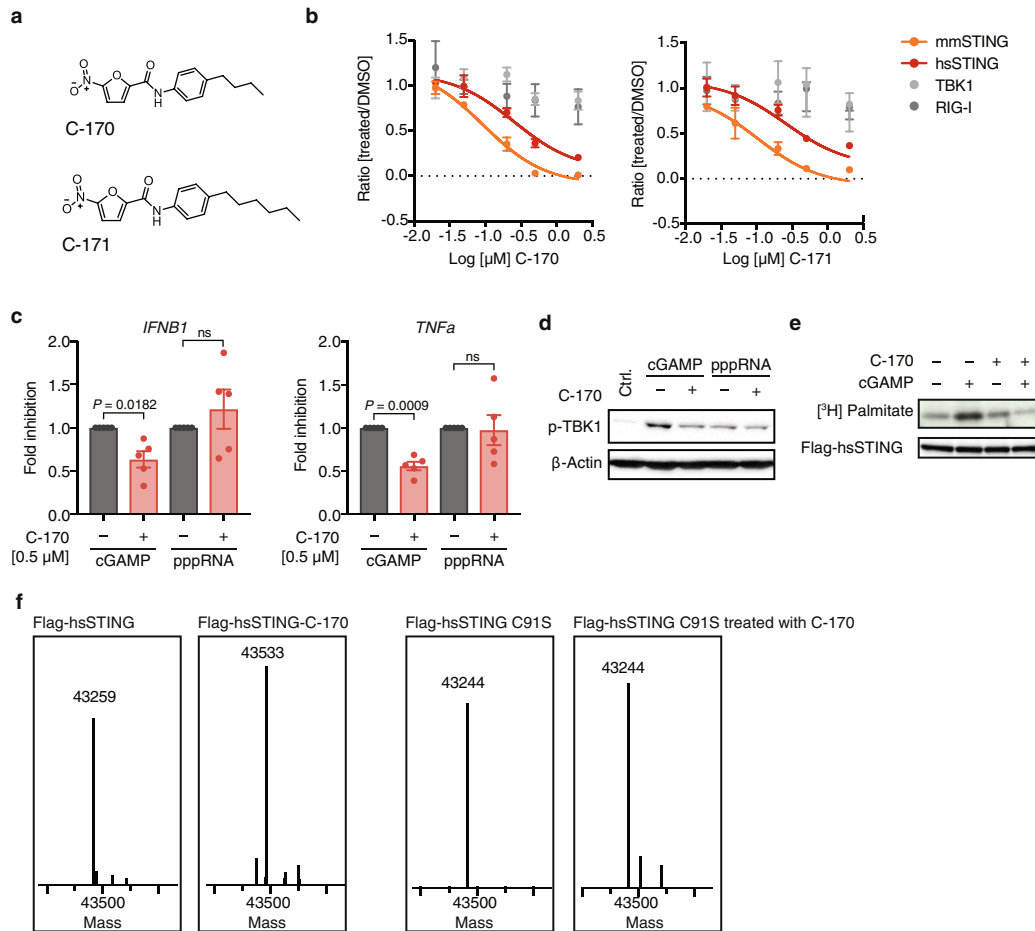
a, Labelling of endogenous STING immunoprecipitated from splenocytes of mice treated with C-176-AL, visualized by in-gel fluorescence. One representative of $n = 2$. **b**, Plasma concentration profiles of C-176 after a single-dose intraperitoneal injection into wild-type mice ($n = 2$ mice per condition). Data are mean \pm s.d. of technical replicates. **c**, Serum levels of type I IFNs and IL-6 from wild-type mice pretreated with C-176 or vehicle 4 h after injection with CMA ($n = 3$ mice per condition). **d**, Body weight of

wild-type mice during two weeks of daily DMSO and C-176 injection. **e–g**, Mice from **d** were euthanized and blood samples were collected for measuring plasma levels of TNF α and IL-6 (**e**), blood cell counts (**f**), and liver and kidney parameters (**g**). Data are mean \pm s.d. of $n = 10$ mice per condition (**e–g**). *P* values were calculated by one-way ANOVA (**c**) or two-tailed *t*-test (**e–g**). ns, not significant. For gel source data, see Supplementary Fig. 1. For source data, see Supplementary Table 1.



Extended Data Fig. 7 | Activity of C-178 and C-176 in TREX1-deficient cells and mice. **a**, Wild-type ($n = 2$) or *Trex1*^{-/-} ($n = 7$) mouse embryonic fibroblasts were treated with DMSO or C-178 (2 μ M) overnight. mRNA levels of *Isg15* and *Cxcl10* were measured by RT-qPCR. **b**, **c**, Control mice (wild type or *Trex1*^{+/-} (each $n = 3$)) were treated with vehicle, and *Trex1*^{-/-} mice were treated with C-176 ($n = 5$ mice) or vehicle ($n = 4$ mice) for 11 days. Serum type I IFN levels (**b**) were measured and histological

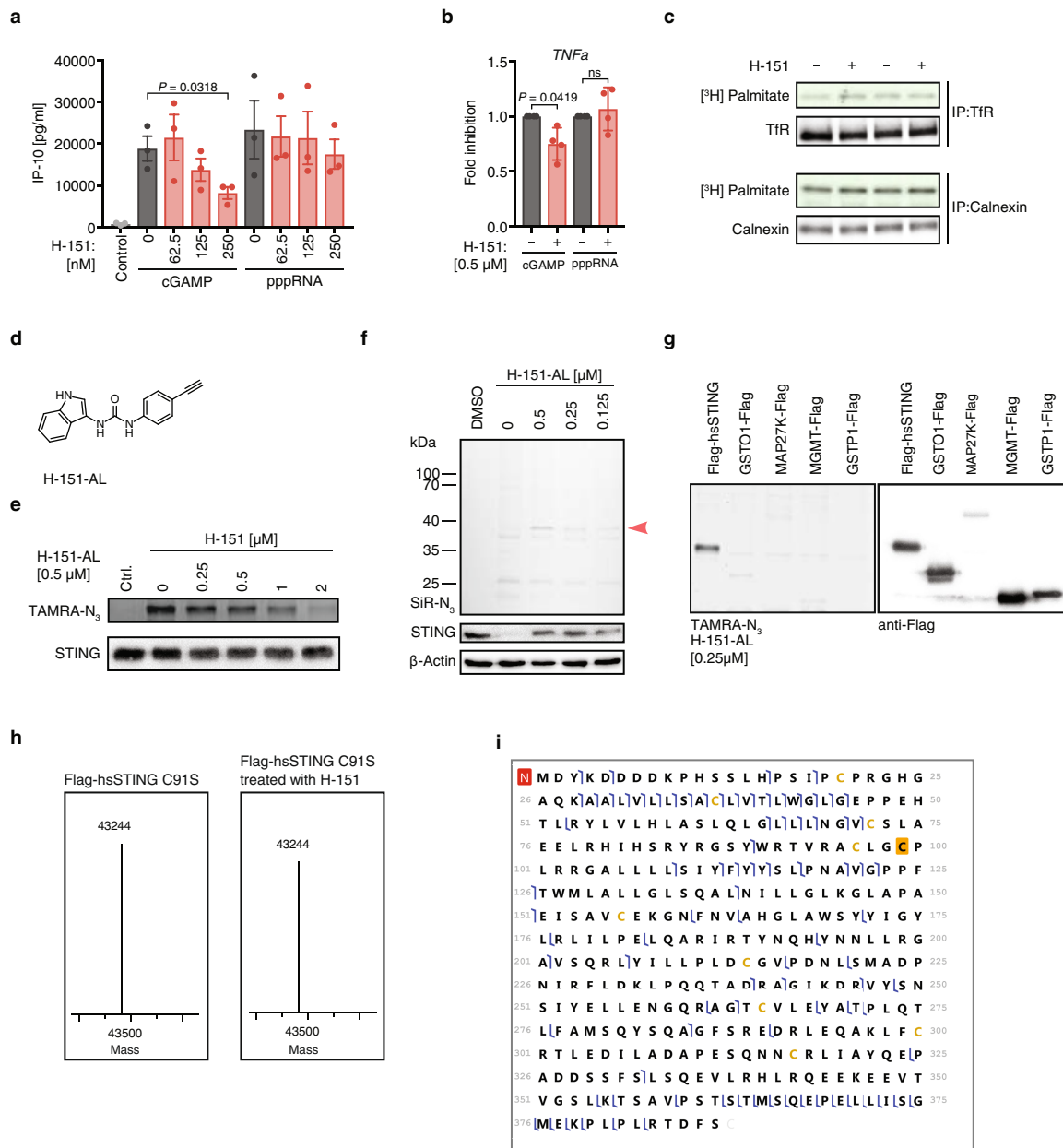
analysis of the heart (**c**) was performed. Scale bars, 50 μ m. **d**, Histological analysis of distinct organs from wild-type (all $n = 4$) or *Trex1*^{-/-} mice treated for 3 months. Smooth muscle, $n = 3$ (C-176) or 5 (vehicle); tongue and stomach, $n = 3$ (C-176) or 6 (vehicle). Representative histological images are shown. Data are mean \pm s.e.m. P values were calculated using two-tailed t -test (**a**) or one-way ANOVA (**b–d**). For source data, see Supplementary Table 1.



Extended Data Fig. 8 | C-170 and C-171 antagonize hsSTING.

a, Structure of C-170 and C-171. **b**, IFN β luciferase reporter measurements from HEK293T cells transfected with indicated constructs (C-170 and C-171, 0.02–2 μ M) ($n = 3$). **c**, **d**, THP-1 cells were pretreated with C-170 (0.5 μ M) and stimulated with cGAMP or triphosphate RNA. *IFN β* and *TNF α* mRNA levels were assessed by RT-qPCR ($n = 5$) (**c**), and p-TBK1 was determined by immunoblot (**d**). **e**, [3 H]-palmitate labelling of HEK293T cells that express Flag-hsSTING, treated with C-170 (1 μ M) or DMSO. **f**, HEK293T cells that express Flag-hsSTING (wild-type

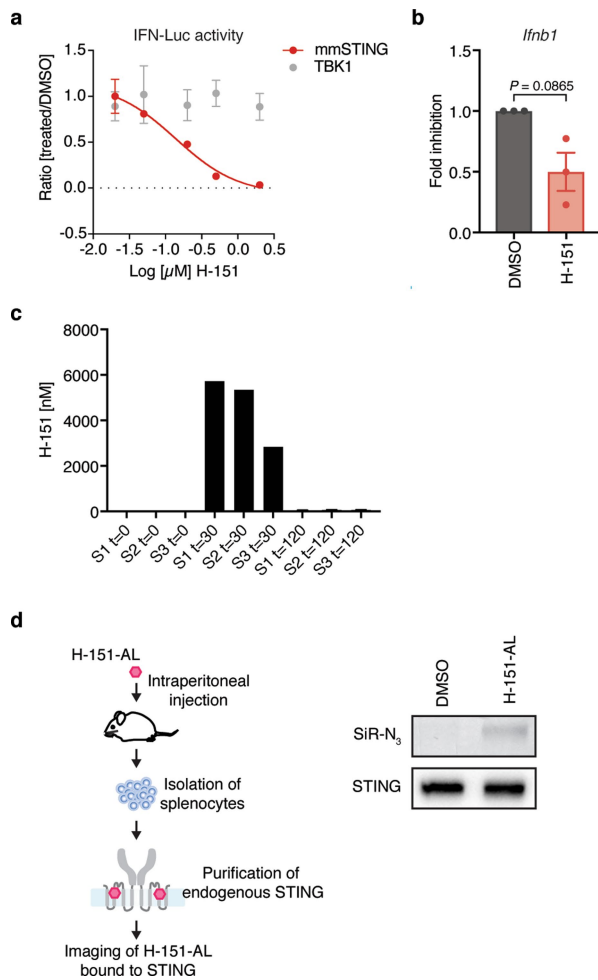
hsSTING or hsSTING(C91S)) were treated with C-170 (1 μ M), lysed and Flag-hsSTING was analysed by intact mass measurement (LC-MS). Deconvoluted electrospray ionization mass spectrum showing intact mass indicated hsSTING constructs and treatments, are shown. Data are mean \pm s.e.m. P values were calculated using two-tailed t -test. NS, not significant. One representative of $n = 3$ (**d**) and $n = 2$ (**e–f**) independent experiments is shown. For gel source data, see Supplementary Fig. 1. For electrospray ionization spectra see Supplementary Information.



Extended Data Fig. 9 | Mechanism of STING inhibition by H-151.

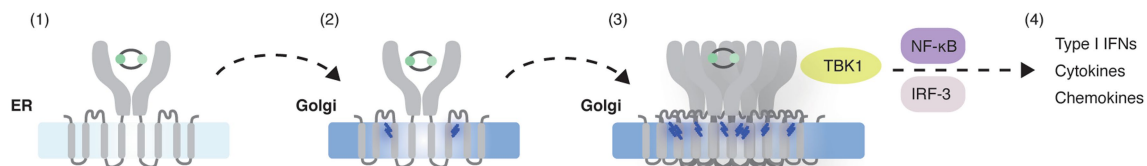
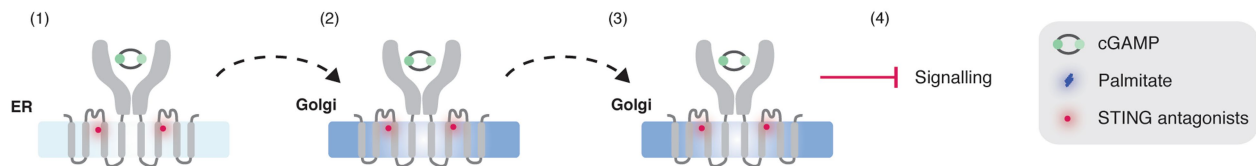
a, THP-1 cells that had been pretreated with H-151 or DMSO were stimulated with cGAMP or triphosphate RNA, or left unstimulated. IP-10 production was quantified by enzyme-linked immunosorbent assay after overnight incubation ($n = 3$). **b**, Levels of *TNF* mRNA assessed by RT-qPCR in THP-1 cells that had been pretreated with H-151 and stimulated with cGAMP or triphosphate RNA ($n = 4$). **c**, [³H]-palmitate labelling of immunoprecipitated endogenous calnexin or transferrin receptor from HEK293T cells that had been treated with H-151 (1 μM). **d**, Structure of H-151-AL. **e**, Competition assay of H-151-AL with H-151 in HEK293T cells that express Flag-hsSTING. Flag-hsSTING labelled with H-151-AL was visualized by in-gel fluorescence. **f**, HEK293T cells or HEK293T cells that express Flag-hsSTING were treated with H-151-AL, lysed and clicked to a SiR azide. Whole-cell lysates were analysed by in-gel fluorescence and by immunoblot. **g**, HEK293T cells that express Flag-

hsSTING, GSTO1-Flag, MAP27K-Flag, MGMT-Flag or GSTP1-Flag were exposed to H-151-AL, clicked to TAMRA azide and visualized by in-gel fluorescence or immunoblot. **h**, Deconvoluted electrospray ionization mass spectrum showing intact mass of Flag-hsSTING(C91S) with or without H-151. **i**, Flag-hsSTING was purified from HEK293T cells that had been pretreated with H-151 (1 μM) and analysed by top-down analysis using LC-HCD-MS/MS (with additional 8 residues due to N-terminal Flag). Data that were obtained with three different NCE values are combined to create fragmentation map with assigned *b*- and *y*-fragments. Achieved sequence coverage is 23% with 20 p.p.m. mass accuracy for fragment assignment. Data are shown as mean \pm s.e.m. *P* values were calculated by two-tailed *t*-test. NS, not significant. One of $n = 2$ experiments is shown (**c**, **e**-**h**). For gel source data, see Supplementary Fig. 1. For electrospray ionization spectra, see Supplementary Information.



Extended Data Fig. 10 | Activity of H-151 against mmSTING.

a, HEK293T cells were transfected with plasmids encoding mmSTING in combination with cdG-Syn or were transfected with a plasmid for TBK1, and an IFN β luciferase reporter, and then treated with H-151 (concentration 0.02–2 μ M). Reporter activity was measured after overnight incubation. Data are mean \pm s.e.m. ($n = 3$; nonlinear regression analysis). Experiments were performed together with those that generated the data displayed in Fig. 5b. **b**, BMDMs were pretreated with H-151 (0.5 μ M) and levels of *Ifnb1* mRNA expression induced by cGAMP were assessed by RT-qPCR. Data are mean \pm s.e.m. ($n = 3$); P value was calculated by two-tailed t -test. **c**, Mean plasma concentration profiles of H-151 following a single-dose intraperitoneal injection into wild-type mice ($n = 3$ mice per time point). **d**, Schematic, and in vivo detection of H-176-AL binding to mmSTING. Visualization by in-gel fluorescence was performed using SiR azide. One representative of $n = 2$. For gel source data, see Supplementary Fig. 1. For source data, see Supplementary Table 1.

Intact STING signalling*Small-molecule mediated inhibition*

Extended Data Fig. 11 | Mechanism of action of the identified STING antagonists. In the absence of inhibition, ligand binding triggers the translocation of STING to the Golgi^{1,25}, where palmitoylation occurs at cytoplasmic proximal cysteine residues (Cys88 and Cys91)²⁶. In turn, this post-translational modification facilitates the multimerization of

STING to create a platform—possibly at the lipid raft domain at the trans-Golgi network²⁶—for the recruitment of TBK1, and thereby enables the initiation of downstream signalling. Through covalent interaction with Cys91, the compounds we describe here block the palmitoylation of STING and retain the protein in a signalling-incompetent state.

Reporting Summary

Nature Research wishes to improve the reproducibility of the work that we publish. This form provides structure for consistency and transparency in reporting. For further information on Nature Research policies, see [Authors & Referees](#) and the [Editorial Policy Checklist](#).

Statistical parameters

When statistical analyses are reported, confirm that the following items are present in the relevant location (e.g. figure legend, table legend, main text, or Methods section).

n/a Confirmed

- The exact sample size (n) for each experimental group/condition, given as a discrete number and unit of measurement
- An indication of whether measurements were taken from distinct samples or whether the same sample was measured repeatedly
- The statistical test(s) used AND whether they are one- or two-sided
Only common tests should be described solely by name; describe more complex techniques in the Methods section.
- A description of all covariates tested
- A description of any assumptions or corrections, such as tests of normality and adjustment for multiple comparisons
- A full description of the statistics including central tendency (e.g. means) or other basic estimates (e.g. regression coefficient) AND variation (e.g. standard deviation) or associated estimates of uncertainty (e.g. confidence intervals)
- For null hypothesis testing, the test statistic (e.g. F , t , r) with confidence intervals, effect sizes, degrees of freedom and P value noted
Give P values as exact values whenever suitable.
- For Bayesian analysis, information on the choice of priors and Markov chain Monte Carlo settings
- For hierarchical and complex designs, identification of the appropriate level for tests and full reporting of outcomes
- Estimates of effect sizes (e.g. Cohen's d , Pearson's r), indicating how they were calculated
- Clearly defined error bars
State explicitly what error bars represent (e.g. SD, SE, CI)

Our web collection on [statistics for biologists](#) may be useful.

Software and code

Policy information about [availability of computer code](#)

Data collection

In-gel fluorescence data were acquired by Fusion capt advance acquisition software. Western blots were acquired using Image Lab software (Biorad). RT-qPCR data were acquired using QuantStudio 5 Real-Time PCR system (ThermoFisher). Microscopic images were acquired using ZEN 2009 (Zeiss) software using Zeiss LSM710. Blood plasma parameters were measured using Dimension Xpand Plus (Siemens Healthcare Diagnostics AG). Blood counts were collected using ADVIA120 hematology system (Siemens Healthcare Diagnostics AG). Luciferase activity in supernatants and absorbance measurements was measured using TECAN Spark 10M or TECAN infinite plate reader. Western Blot images were analysed using Image Lab (Biorad). ECL signal was recorded using ChemiDoc XRS Biorad Imager.

Data analysis

Microscopic images were analysed by ImageJ. MS data were deconvoluted using MagTran 1.03 software or Protein Deconvolution (Thermo Fischer Scientific) using Respect algorithm. Top-down data were deconvoluted using MASH Suite software (Ge research group, University of Wisconsin) and fragmentation maps were generated using ProSight Lite software (Kelleher research group, Northwestern University). Statistical analysis and graph design was performed using Prism 6 and 7. HPLC data were analysed by Chromeleon (Dionex). For the in vivo measurement of Luciferase activity, photon flux was quantified on an In-vivo Xtreme II imaging device (Bruker). Western Blot images were analysed using Image Lab (Biorad). Autoradiography was quantified using Typhoon Imager (ImageQuantTool, GE Healthcare). In-gel fluorescence was analysed using Fusion capt advance acquisition software.

For manuscripts utilizing custom algorithms or software that are central to the research but not yet described in published literature, software must be made available to editors/reviewers upon request. We strongly encourage code deposition in a community repository (e.g. GitHub). See the Nature Research [guidelines for submitting code & software](#) for further information.

Data

Policy information about [availability of data](#)

All manuscripts must include a [data availability statement](#). This statement should provide the following information, where applicable:

- Accession codes, unique identifiers, or web links for publicly available datasets
- A list of figures that have associated raw data
- A description of any restrictions on data availability

RNA sequencing data have been deposited in the Gene Expression Omnibus (GEO) under the accession code (GSE113933). Full scans for all western blots and in-gel fluorescence images are provided in Supplementary Fig. 1. Source data for animal experiments from Fig. 4, 5g, h, i and Extended Data Fig. 6b-g, 7b-d and 10c are shown in Supplementary Table 1. All other data are available from the corresponding author on reasonable request.

Field-specific reporting

Please select the best fit for your research. If you are not sure, read the appropriate sections before making your selection.

Life sciences Behavioural & social sciences Ecological, evolutionary & environmental sciences

For a reference copy of the document with all sections, see nature.com/authors/policies/ReportingSummary-flat.pdf

Life sciences study design

All studies must disclose on these points even when the disclosure is negative.

Sample size	We have used at least three biological replicates for each experiment - unless stated otherwise. This is consistent with previous studies and accounts for biological variability in between distinct samples from inbred mice or from cell lines. No statistical method was used to predetermine sample size.
Data exclusions	There were no data excluded from the study.
Replication	Experimental findings were reliably reproduced. The number (n) of biological replicates or animals is indicated as an exact number in the figure legends.
Randomization	Mice were randomly allocated to distinct groups.
Blinding	Experimenters were blinded for the analysis of the histopathological scores.

Reporting for specific materials, systems and methods

Materials & experimental systems

n/a	Involved in the study
<input type="checkbox"/>	<input checked="" type="checkbox"/> Unique biological materials
<input type="checkbox"/>	<input checked="" type="checkbox"/> Antibodies
<input type="checkbox"/>	<input checked="" type="checkbox"/> Eukaryotic cell lines
<input checked="" type="checkbox"/>	<input type="checkbox"/> Palaeontology
<input type="checkbox"/>	<input checked="" type="checkbox"/> Animals and other organisms
<input checked="" type="checkbox"/>	<input type="checkbox"/> Human research participants

Methods

n/a	Involved in the study
<input checked="" type="checkbox"/>	<input type="checkbox"/> ChIP-seq
<input checked="" type="checkbox"/>	<input type="checkbox"/> Flow cytometry
<input checked="" type="checkbox"/>	<input type="checkbox"/> MRI-based neuroimaging

Unique biological materials

Policy information about [availability of materials](#)

Obtaining unique materials

Antibodies

Antibodies used

WB), anti-Flag M2 (F3165, Sigma 1:2000 WB, 1:500 IF), anti-rabbit-IgG-HRP (Santa Cruz Biotechnology 1:2000 WB), anti-mouse-IgG-HRP (Santa Cruz Biotechnology 1:2000 WB), anti-GM130 (clone 35, BD Pharmingen 1:100 IF), anti- β -actin (C4, Santa Cruz 1:5000 dilution), donkey anti-mouse Alexa Fluor 568 conjugate (ThermoScientific 1:5000 IF), anti-hsSTING (AF6516, RD System, IP) and anti-calnexin (Millipore MAB3126).

Validation

Antibodies used in this study were validated using cellular assays based on overexpression or knockout and knockdown methods or we relied on the target validation stated by the manufactures.

Eukaryotic cell lines

Policy information about [cell lines](#)

Cell line source(s)

MEFs were generated from individual embryos from the respective genotype. BMDMs were prepared from the bone marrow of C57BL/6 mice. WI-38 cells were purchased from ATCC (ATCC-CCL-75). THP-1 cells were obtained from Angela Rösen-Wolff, University Hospital Dresden, Germany, HEK293T cells from Didier Trono, EPFL, Switzerland.

Authentication

MEFs were identified by genotyping. For other cells no methods was used for authentication.

Mycoplasma contamination

All cell lines were routinely tested for mycoplasma by PCR and were used mycoplasma-free.

Commonly misidentified lines
(See [ICLAC](#) register)

No commonly misidentified cell lines were used in this study.

Animals and other organisms

Policy information about [studies involving animals](#); [ARRIVE guidelines](#) recommended for reporting animal research

Laboratory animals

For experiments assessing the short-term effect of the compounds against exogenous STING stimulation, C57BL/6J mice were used at an age of 8 - 12 weeks. Trex1^{-/-} mice (backcrossed for > 10 generations to C57BL/6NJ) and corresponding Trex1^{+/-}, Trex1^{+/+} were used at an age of 2-5 weeks. Trex1^{-/-} IFN-beta-luc-reporter mice were used at an age of 4-7 weeks.

Wild animals

The study did not involve wild animals.

Field-collected samples

The study did not involve field-collected samples.